

# MicroRNA-122-5p inhibits inflammation and fibrosis in mice with acute pancreatitis through upregulation of APOE level by binding to HDAC1

Lu Yan<sup>1,2</sup>, Jie Peng<sup>1</sup>, Meng Wang<sup>1</sup>, Zimeng Guo<sup>1</sup>, Haosu Huang<sup>1</sup>, Huan Gu<sup>1,2</sup>

<sup>1</sup>Department of Gastroenterology, Xiangya Hospital, Central South University, Changsha, China

<sup>2</sup>National Clinical Research Center for Geriatric Disorders, Xiangya Hospital, Changsha, China

Submitted: 26 August 2022; Accepted: 10 January 2023

Online publication: 20 January 2023

Arch Med Sci

DOI: <https://doi.org/10.5114/aoms/159179>

Copyright © 2023 Termedia & Banach

Corresponding author:

Huan Gu

Xiangya Hospital

Central South University

Xiangya, China

E-mail: [Guhuan83@csu.edu.cn](mailto:Guhuan83@csu.edu.cn)

## Abstract

**Introduction:** This research was designed to ascertain the mechanism of miR-122-5p in alleviating the inflammation and fibrosis of mice with acute pancreatitis (AP).

**Material and methods:** The AP mouse or cell model was established by caerulein (CAE) treatment. The pancreatic coefficient was evaluated and the expression levels of amylase (AMS) and lipase were measured using a kit. The pathological changes of pancreatic tissues were observed under hematoxylin-eosin (H&E) staining. The expression levels of fibrous proteins ( $\alpha$ -SMA and collagen I) were detected. The expression levels of related inflammatory factors (IL-1 $\beta$ , IL-6, and TNF- $\alpha$ ) were tested by ELISA. The correlations between miR-122-5p and histone deacetylase 1 (HDAC1) or between HDAC1 and apolipoprotein E (APOE) were predicted and validated.

**Results:** In AP mice or cells, the pancreatic coefficient was elevated ( $p < 0.01$ ), and the AMS expression was increased ( $p < 0.001$ ) while lipase expression was decreased ( $p < 0.05$ ). The pathological structural change was obvious and the Rongione score was elevated ( $p < 0.001$ ). The expression of  $\alpha$ -SMA and collagen I was stimulated ( $p < 0.05$ ), and the levels of IL-1 $\beta$ , IL-6, and TNF- $\alpha$  were enhanced ( $p < 0.001$ ). miR-122-5p negatively regulated HDAC1 expression and HDAC1 inhibited APOE transcription. Overexpression of miR-122-5p or APOE could both reduce the inflammation and fibrosis in AP mice or cells but upregulation of HDAC1 or APOE inhibition reversed the inhibiting effect of miR-122-5p overexpression on CAE-induced inflammation and fibrosis.

**Conclusions:** miR-122-5p inhibited inflammation and fibrosis in an AP mouse model by the HDAC1/APOE axis.

**Key words:** miR-122-5p, HDAC1, APOE, inflammation, fibrosis, acute pancreatitis.

## Introduction

Pancreatitis, a digestive tract disease caused by the self-digestion of trypsin in the pancreas, is mainly divided into acute pancreatitis (AP) and chronic pancreatitis (CP) [1]. The progression of a sentinel attack of AP to CP is often driven by bile stones, excessive use of alcohol, or genetic risk factors [2]. Acute pancreatitis is a severe pancreatic inflammatory condition that occurs suddenly and often with severe abdominal pain, which leads to high mortality if accompanied by severe local and systemic complications [3]. Evidence showed that uncontrolled or dysregulated activa-

tion of the immune system can contribute to the excessive systemic inflammation associated with AP [4]. Therefore, extensive exploration of mechanisms behind the inflammatory response in AP is a valuable adjunct for the disease management.

MicroRNAs (miRs) are small endogenous RNAs that regulate gene expression post-transcriptionally [5]. Several miRs are reported to be involved in facilitating the development of chronic inflammation by modulating tissue-infiltrated immune cell function [6]. A previous study showed that a panel of serum miRs (including miR-122-5p) could serve as a non-invasive biomarker for the early detection of pancreatic ductal adenocarcinoma (PDAC) [7]. For example, miR-122-5p was reported to play an important role in suppressing cell biological phenotypes and epithelial-mesenchymal transition by downregulating cyclin G1 in PDAC [8]. Also, miR-122-5p could serve as a potential biomarker of liver fibrosis in patients with hepatitis B virus (HBV)-associated fibrosis [9]. In an animal experiment of tubulointerstitial fibrosis, miR-122-5p was significantly decreased in aristolochic acid-induced acute nephropathy [10]. However, molecular mechanisms modulated by miR-122-5p in AP remain largely undiscovered.

Histone deacetylase 1 (HDAC1) plays a vital role in transcriptional regulation in eukaryotic cells and associates with proteins, i.e. transcription factors, coactivators, chromatin remodeling proteins and so on, during development [11]. Notably, aberrantly expressed HDAC1 has been frequently studied in human cancers. Research by Lai *et al.* revealed that HDAC1 may participate in the progression of renal fibrosis [12]. Moreover, HDAC1 was highly expressed in cardiac fibroblasts [13]. Interestingly, the binding of HDAC1 and apolipoprotein E (APOE) was documented in the University of California Santa Cruz (UCSC) database. Apolipoprotein E is responsible for the uptake of lipoproteins and linked with the risk of cystic fibrosis dyslipidemia [14]. Another study revealed that lack of APOE aggravated liver fibrosis in mice [15], which indicated that the expression of APOE may regulate the fibrosis process.

Reportedly, HDAC modulated the transcription of miR-15/16, which then regulated the apoptosis and fibrosis of pancreatic stellate cells in pancreatitis [16]. Another study reported that the interaction between miR-383 and APOC3 may affect pancreatic apoptosis in high-fat induced diabetic mice [17]. In accordance with the previous research results, we intended to explore the interaction between HDAC1/APOE and miRs in AP. Through bioinformatics prediction, HDAC1 was identified as a putative target of miR-122-5p. Therefore, we speculated that miR-122-5p might affect AP via HDAC1/APOE. To validate this hypothesis, we

conducted experiments to investigate the specific mechanisms of miR-122-5p in AP by targeting downstream genes.

## Material and methods

### Animals

Ninety-six male healthy BALB/c mice (6 weeks old,  $20 \pm 2$  g, Beijing Vital River Laboratory Animal Technology Co., Ltd.) were fed in a specific pathogen-free (SPF) sterile laminar flow chamber under a 12-h dark/light cycle at a constant temperature of 21–25°C and a constant humidity of 50–65% with free access to food and water for one week. All operations were conducted under the approval of the animal ethics committee of the local hospital.

### Establishment of the acute pancreatitis mouse model

In accordance with the methods developed by Wang *et al.* [18], BALB/c mice were fasted for 12 h but provided with water, and the experimental mice were intraperitoneally administered 50 µg/kg caerulein (CAE; C9026, sigma, Sigma-Aldrich, St. Louis, MO, USA) once an hour for 7 times in total. The mice were euthanized 24 h after the last injection of CAE, and serum and pancreatic tissue samples were collected for follow-up experiments.

### Grouping

The mice were grouped into control, AP, miR-122-5p agomir, agomir negative control (NC), over-expression (oe)-HDAC1, short hairpin (sh)-HDAC1, sh-NC, oe-APOE, oe-NC, miR-122-5p agomir + oe-HDAC1, miR-122-5p agomir + oe-NC, oe-HDAC1 + oe-APOE, oe-HDAC1 + oe-NC, agomir NC + sh-NC, miR-122-5p agomir + sh-NC, and miR-122-5p agomir + sh-APOE groups ( $n = 6$  per group). Mice were injected with 10 nmol of adenovirus vectors 24 h before modeling.

### Collection of serum and pancreatic tissue specimens

After the last injection of CAE, mice were weighed, and blood was collected from their orbits. The serum was separated, placed at room temperature for 30 min, centrifuged (3000 r/min, 4°C) for 15 min, aliquoted, and stored in a refrigerator (–80°C). Next, the mice were euthanized to collect and weigh the pancreas. The pancreatic coefficient was calculated as pancreatic wet weight (mg)/mouse weight (g). Then, the pancreas was completely separated by removing the mesentery around the pancreas. The pancreatic tail was divided into three parts for detection of related indi-

ces, pathological evaluation by hematoxylin-eosin (H & E) staining, and fibrosis detection by Masson staining.

#### Hematoxylin-eosin staining

After fixation by paraformaldehyde (4%), the pancreatic tissues were dehydrated with an alcohol gradient (70%, 80%, and 90% alcohol for 1 h, and 95% and 100% alcohol for 2 × 1 h). Subsequently, the tissues were permeabilized in xylene, embedded, and sliced. Next, the slices were dehydrated with conventional gradient alcohol, permeabilized in xylene, and rinsed in distilled water. Then the slices were stained with hematoxylin solution for 3–5 min and washed with distilled water again. After that, the slices were differentiated with 1% alcohol hydrochloric acid for 20 s, followed by treatment with 1% ammonia solution for 30 s and washing in distilled water. The slices were counterstained with 1% eosin solution for 5 min, rinsed with tap water for 5 min and distilled water for 1 min, dehydrated, permeabilized, and sealed. The mounted slides were photographed using a microscope (Tokyo, Japan) for pathological evaluation.

#### Pathological examination of the pancreas

Based on the histological scoring system reported by Rongione *et al.* [19], pancreatic tissue injury was evaluated from 0 to 4 for the severity of edema, hemorrhage, necrosis, inflammation, and vacuolization. The total score of the pathological evaluation was the sum of the scores of the five aspects, and higher score represented more serious injury. Three fields at a high magnification (× 400) were randomly selected and scored, and the mean was calculated.

#### Detection of amylase and lipase

The determination of amylase (AMS) and lipase in pancreatic tissue was performed using an AMS kit (20100215) or lipase kit (20140117) from Nanjing Jiancheng Bioengineering Institute. The homogenates of the pancreatic tissues were centrifuged for 15 min at 300 r/min and 4°C using a refrigerated centrifuge, and the supernatant was gathered to detect AMS and lipase levels based on the kit instructions.

#### Masson staining

Pancreatic tissues were fixed with Zenker's solution for 12 h after being sliced and dewaxed. Then the slices were washed in water with mercury and iodine removed, stained with acid fuchsin solution for 5–10 min, and rinsed with 0.05% glacial acetic acid. After 5-min treatment with 1% phosphomo-

lybdic acid, the slices were redyed with aniline blue (5 min), rinsed in 1% glacial acetic acid (1 min), dehydrated with alcohol, permeabilized with xylene, and sealed. Three fields were selected to observe and analyze the staining results. Collagen fibers were stained blue and muscle cells were stained red. The changes in the amount of collagen fibers were represented by the shades of blue.

#### Acute pancreatitis cell model

HPDE cells (Procell Life Science & Technology Co., Ltd., Wuhan, China) were cultured in Dulbecco's Modified Eagle Medium (Gibco, Grand Island, NY, USA) supplemented with 10% fetal bovine serum (Thermo Fisher Scientific, Wilmington, DE, USA) and antibiotic (Gibco, Grand Island, NY, USA) at 37°C in an atmosphere of 5% CO<sub>2</sub>. After 6-h culture, cells were digested with trypsin, subcultured, and then inoculated in medium for 24 h. After that, 100 nM CAE was added for co-incubation for 24 h, and then the cells were collected.

#### Cell transfection

Overexpression vectors of miR-122-5p, APOE, and HDAC1 (miR-122-5p agomir, oe-APOE, and oe-HDAC1), knockdown vector of APOE (sh-APOE), and their NCs were all acquired from GenePharma (Shanghai, China). Cell transfection was performed for 48 h based on the instructions with the Lipofectamine 2000 kit (Invitrogen, Carlsbad, CA, USA) into HPDE cells at passage 3 (P3).

#### ELISA

The expression levels of inflammatory factors (IL-1β, TNF-α, and IL-18) were determined following the manuals of ELISA kits (R&D Systems, UK). Specifically, 100 μl samples or standard were added to the wells and incubated in an incubator at 37°C for 90 min. Then the specific antibody was added for 60 min and avidin-biotin-peroxidase complex (ABC) diluent was added for 30 min. Finally, 3,3',5,5'-tetramethylbenzidine was added for incubation for 20–25 min. The absorbance value was measured at a wavelength of 450 nm on a microplate reader.

#### Immunohistochemistry

The isolated pancreatic tissue was fixed with 4% paraformaldehyde for 48 h and then cut into 4-μm paraffin slices. After baking for 20 min, the slices were dewaxed with conventional xylene, washed once with distilled water and 3 times with PBS, and maintained with 3% H<sub>2</sub>O<sub>2</sub> for 10 min. Next, the slices were washed with PBS before antigen repair. After 3 more times of PBS washing, the slices were treated with normal goat serum

blocking solution for 20 min. The primary antibodies collagen I (72026S, 1:100, Cell Signaling Technology, CST, Boston, USA) and  $\alpha$ -SMA (56856S, 1:250, CST) were added and incubated at 4°C overnight. Afterwards, the slices were washed 3 times with PBS and the secondary antibody was added and incubated at room temperature for 1 h. Following three times of PBS washing, the slices were stained with DAB for 1–3 min for color development. The slices were stained with hematoxylin for 3 min, dehydrated, cleared, and sealed. Three fields were selected for observation under a microscope ( $\times 200$ ) and Image J software was used for immunohistochemistry (IHC) staining analysis. The percentage of positive cells and the intensity of staining in the micrographs were scored using semi-quantitative results. The percentage of positive cells was scored as follows: 0 points, < 5%; 1 point, 5-25%; 2 points, 26-50%; 3 points, 51-75%; 4 points, 76-100%. The staining intensity was scored as follows: 0 points, colorless; 1 point, light yellow; 2 points, brown-yellow; 3 points, dark brown. The product of the two scores was the positive grade: 0, negative; 1–4, weakly positive; 5–8, positive; 9–12, strongly positive.

#### Quantitative real-time polymerase chain reaction (qRT-PCR)

Mouse pancreatic tissues and AP cells were collected and total RNA was extracted using Trizol.

**Table 1.** Primer sequences used for quantitative real-time polymerase chain reaction

Name of primer	Sequences (5'-3')
miR-122-5p-F-mus	TATTCGCACTGGATACGACACAAC
miR-122-5p-R-mus	GCCCCGTGGAGTGTGACAATGGT
miR-122-5p-F-hsa	ACACTCCAGCTGGGAA
miR-122-5p-R-hsa	GTGCAGGGTCCGAGGT
HDAC1-F-mus	TGAAGCCTCACCGAATCCG
HDAC1-R-mus	GGGCGAATAGAACGCAGGA
HDAC1-F-hsa	CTGCTAAAGTATCACCAGAGGGT
HDAC1-R-hsa	TGGCCTCATAGGACTCGTCA
ApoE-F-mus	ATTTTCCCTCCGCAGACTGG
ApoE-R-mus	AGTGCCGTCAGTCTTGTGT
APOE-F-hsa	GTTGCTGGTCACATTCCTGG
APOE-R-hsa	GCAGGTAATCCCAAAGCGAC
GAPGH-F-mus	CCTGCCTCTACTGGCGCTGC
GAPDH-R-mus	GCAGTGGGGACACGGAAGGC
GAPGH-F-hsa	GGTGAAGGTCGGAGTCAACG
GAPDH-R-hsa	TGAAGGGTCATTGATGGCAAC
U6-F	CTCGCTTCGGCAGCACA
U6-R	AACGCTTACGAATTTGCGT

F – forward, R – reverse.

The RNA purity and concentration were tested using a NanoDrop spectrophotometer and the RNA was reverse transcribed into cDNA in accordance with the kit (TaKaRa, Tokyo, Japan) manuals. Gene expression was measured on a Biosystems 7300 real time PCR system (ABI, Foster City, CA, USA) based on the protocols of a fluorescence quantitative PCR kit (SYBR Green Mix, Takara). Three replicates were set for each reaction of quantitative PCR. The internal reference was U6 or GAPDH and the  $2^{-\Delta\Delta Ct}$  method was adopted for data analysis:  $\Delta\Delta Ct = \text{experimental group (Ct target gene)} - \text{Ct internal control} - \text{control group (Ct target gene)} - \text{Ct internal control}$ . All primers are detailed in Table 1.

#### Western blot

After pancreatic tissues or cells were lysed on ice for 15 min with RIPA lysis buffer (Beyotime) and centrifuged at 13,000g for 5 min, a BCA detection kit (Beyotime) was used to detect the protein concentration. The loading buffer was added to the protein before protein denaturation using a boiling water bath for 10 min. The volume of each sample was calculated according to the protein loading quantity (30  $\mu$ g of protein per lane). After loading, electrophoresis was performed at 80 V for 30 min, and at 120 V for 90 min after bromophenol blue entered the separation gel. Membrane transfer was performed in an ice bath with a current of 250 mA for 100 min, and then the PVDF membrane was washed with washing solution 3 times, each for 1–2 min. After the membranes had been incubated with blocking buffer for 2 h, the primary antibodies of APOE (ab183597, 1:1000, Abcam, Cambridge, MA, USA), HDAC1 (5356S, 1:1000, CST), collagen I (72026S, 1:100, CST),  $\alpha$ -SMA (56856S, 1:250, CST), and GAPDH (5174S, 1:1000, CST) were added for incubation. The membranes were washed with TBST (3  $\times$  10 min), and then a horseradish peroxidase labeled goat anti-rabbit secondary antibody (IgG, A0208, 1:1000, Beyotime) was added for incubation for 2 h at room temperature. After washing (3  $\times$  10 min), the membranes were detected by Bio-Rad and analyzed by Quantity One v4.6.2 software after application of electrochemiluminescence (ECL, P0018FS, Beyotime). The relative protein content was expressed by the ratio of the gray value of the corresponding protein band to the gray value of the GAPDH protein band.

#### ChIP-qPCR

According to manufacturer's protocols, the ChIP assay was performed using the MAGnify ChIP system (Life Technology, Carlsbad, CA, USA). HPDE cells were fixed with 1% formaldehyde to crosslink DNA-protein and protein-protein complexes. After

that, the crosslinking was terminated by adding 1.25 M glycine for 5 min. The cells were lysed, and DNA was fragmented by sonication, and precipitated. Then diluted suspension was cultured with 5 µg of hnRNP-K antibody. The supernatant was diluted at a dilution of × 10 and retained as an “input” for normalization. After washing, the proteins were treated with protease K and cultured at 65°C for de-crosslinking. Subsequently, a qRT-PCR experiment was performed using the purified DNA fragments as amplification templates. Each experiment was repeated in triplicate and then the data were averaged.

#### Dual luciferase reporter gene assay

TargetScan ([http://www.targetscan.org/vert\\_72/](http://www.targetscan.org/vert_72/)) was used to predict the binding site of miR-122-5p with the HDAC1 promoter. As per the predicted results, wild and mutated sequences of the binding site (HDAC1-wt and HDAC1-mut) were designed, synthesized, and inserted into luciferase reporter gene vectors (pGL3-Promotor). Then the sequences were co-transfected into HEK 293T cells with the miR-122-5p mimic or the negative control of the miR-122-5p mimic. Following transfection, the luciferase intensity of each group was tested using the dual luciferase reporter gene detection kit (Promega, Madison, WI, USA) and photometer (Turner BioSystems, USA).

The binding of HDAC1 and APOE promoters was verified based on the above steps of the dual luciferase reporter gene assay, for which the APOE reporter vector and different concentrations of HDAC1 overexpression plasmid (0, 0.5, 1, and 2 µg) were transfected into HEK239T cells.

#### RNA pull-down

Three different biotin-labeled miRNA sequences, including wild-type miR-122-5p (BiomiR-30e-3p-WT), mut-type miR-122-5p (Bio-miR-122-5p-MUT, mutation at the sequence complementarily paired with HDAC2), and the negative control miRNA sequence (Bio-NC, not complementary to HDAC1), were designed and synthesized by GenePharma. The three aforementioned miRNA sequences were transfected. After transfection for 48 h, cells were lysed with lysis buffer and the lysate was collected to obtain protein lysis products. The lysates were incubated with M-280 streptavidin-coated magnetic beads (Sigma, St. Louis, MO, USA) at 4°C for 3 h. Then the magnetic beads were washed successively with ice-cold buffer twice, hypotonic buffer three times, and hypertonic buffer once. Finally, the protein-nucleic acid complex was eluted. Total RNA was extracted with TRIzol and the expression level of HDAC1 was measured by qRT-PCR.

#### Statistical analysis

Data were analyzed using GraphPad Prism 7 and expressed as the mean ± standard deviation. The data between two groups were analyzed using the t-test, and those among multiple groups using one-way analysis of variance with Tukey's multiple comparisons test as post hoc analysis. Statistical significance was set at  $p < 0.05$ .

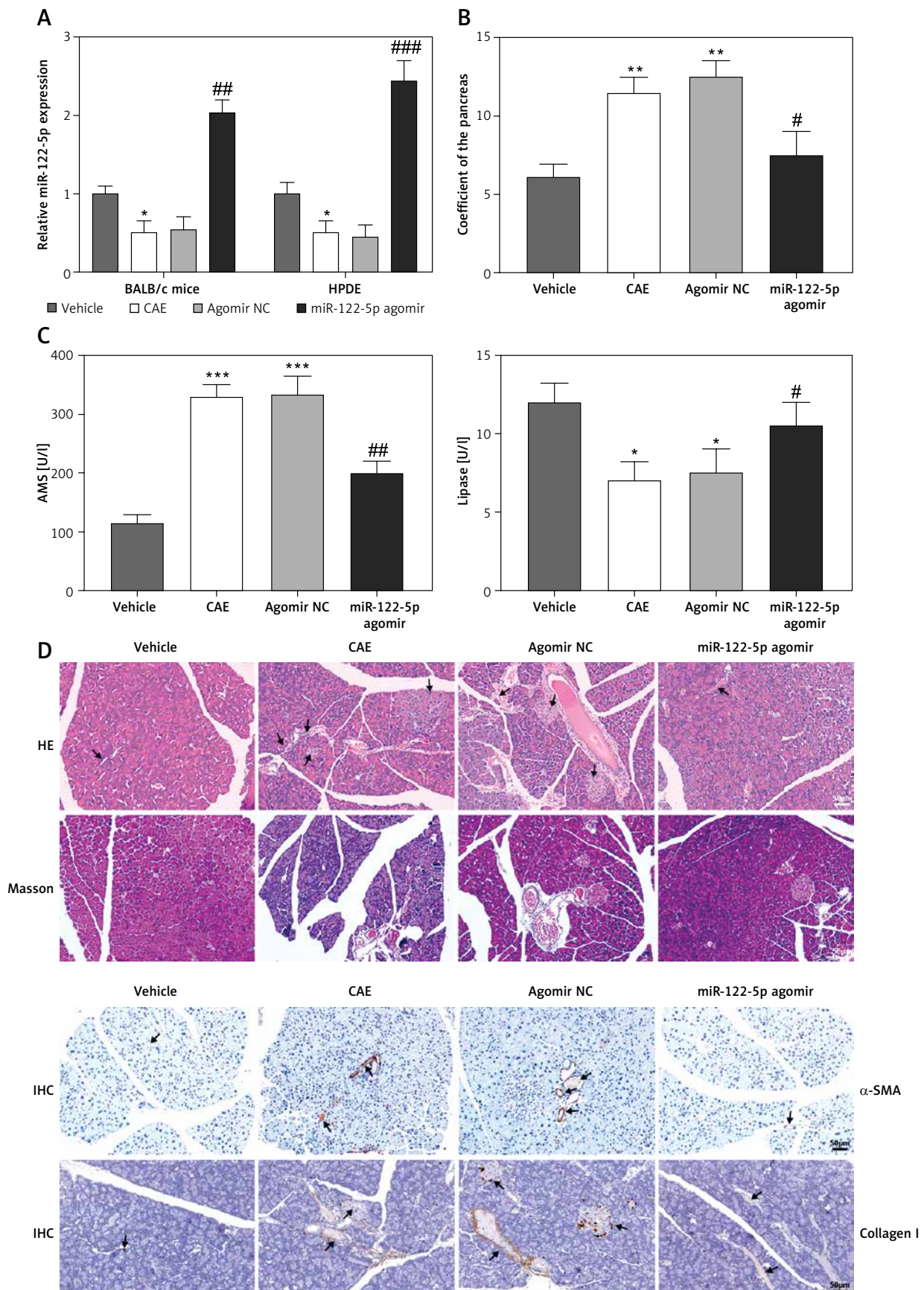
#### Results

##### Overexpression of miR-122-5p relieved inflammation or fibrosis in cells and mice with AP

After AP mouse and cellular models were successfully created by CAE treatment, we used qRT-PCR to measure the expression of miR-122-5p in AP models. The results showed that miR-122-5p was much lower in the CAE group than the vehicle group (Figure 1 A,  $*p < 0.05$ ), which indicated that miR-122-5p played an important role in AP progression. Additionally, miR-122-5p agomir was injected or transfected into AP mice and AP cells, respectively. Results from qRT-PCR showed that miR-122-5p was much higher in the miR-122-5p agomir group than the agomir NC group (Figure 1 A,  $###p < 0.001$ ). Moreover, the pancreatic coefficient was clearly higher in the CAE group compared with vehicle group (Figure 1 B,  $**p < 0.01$ ), while it was clearly lower in the miR-122-5p agomir group compared with the agomir NC group (Figure 1 B,  $#p < 0.05$ ).

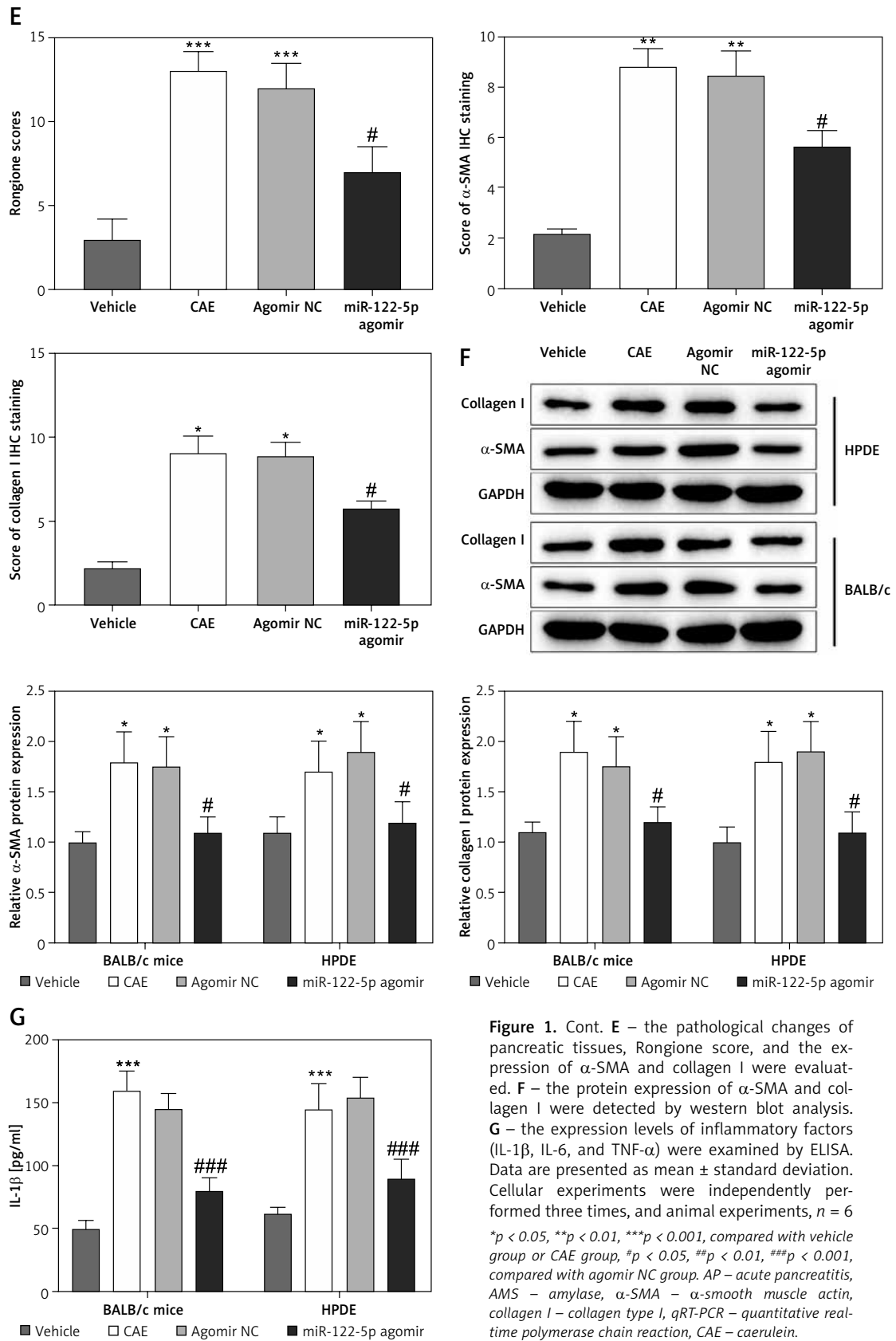
Next, the expression of AMS and lipase in AP mouse pancreatic tissues was tested. The results showed that AMS was significantly stimulated and lipase was significantly inhibited in the CAE group as compared to the vehicle group (Figure 1 C,  $*p < 0.05$ ,  $***p < 0.001$ ). But there was an opposite trend in AMS and lipase levels when miR-122-5p was overexpressed by injection of miR-122-5p agomir (Figure 1 C,  $#p < 0.05$ ,  $##p < 0.01$ ).

In addition, the results from H&E staining showed that the interlobular space of mouse pancreas with AP was widened, concurrent with acinar edema, a patch of necrosis, massive inflammatory cell infiltration in parenchyma and interstitium, scattered red blood cells in the pancreatic tissue; and the Rongione score was markedly increased as compared to the vehicle group (Figures 1 D, E,  $***p < 0.001$ ). In the miR-122-5p agomir group, the histopathological score was substantially reduced and AP-induced injuries were markedly alleviated, i.e. decreased interlobular space in the pancreas and necrosis and alleviated acinar edema (Figures 1 D, E,  $#p < 0.05$ ). Results from Masson and IHC staining showed that the acinar of pancreatic tissue was irregularly arranged, the thickened interstitium was stained blue, and the expression lev-



**Figure 1.** Upregulated miR-122-5p alleviates CAE-induced inflammation or fibrosis in mice and cells. **A** – the expression of miR-122-5p in AP mice and cell was examined by qRT-PCR before or after exposure to miR-122-5p agomir. **B, C** – the pancreatic coefficient was analyzed and the expression levels of AMS and lipase were tested. **D** – the pathological changes of pancreatic tissues, Rongione score, and the expression of  $\alpha$ -SMA and collagen I were evaluated

\* $p < 0.05$ , \*\* $p < 0.01$ , \*\*\* $p < 0.001$ , compared with vehicle group or CAE group, # $p < 0.05$ , ## $p < 0.01$ , ### $p < 0.001$ , compared with agomir NC group. AP – acute pancreatitis, AMS – amylase,  $\alpha$ -SMA –  $\alpha$ -smooth muscle actin, collagen I – collagen type I, qRT-PCR – quantitative real-time polymerase chain reaction, CAE – caerulein.



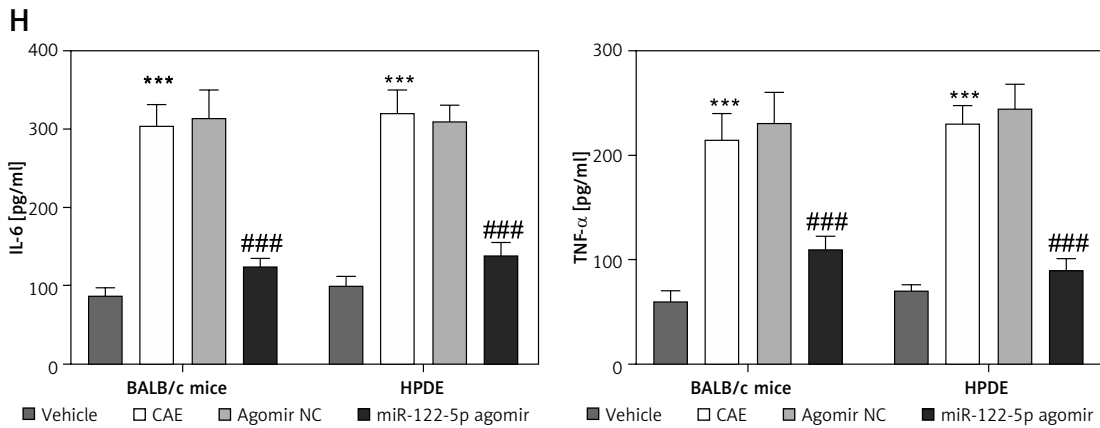


**Figure 1.** Cont. **H** – the expression levels of inflammatory factors (IL-1 $\beta$ , IL-6, and TNF- $\alpha$ ) were examined by ELISA. Data are presented as mean  $\pm$  standard deviation. Cellular experiments were independently performed three times, and animal experiments,  $n = 6$

\* $p < 0.05$ , \*\* $p < 0.01$ , \*\*\* $p < 0.001$ , compared with vehicle group or CAE group, # $p < 0.05$ , ## $p < 0.01$ , ### $p < 0.001$ , compared with agomir NC group. AP – acute pancreatitis, AMS – amylase,  $\alpha$ -SMA –  $\alpha$ -smooth muscle actin, collagen I – collagen type I, qRT-PCR – quantitative real-time polymerase chain reaction, CAE – caerulein.

els of  $\alpha$ -SMA and collagen I were evidently higher in the CAE group, compared with the vehicle group (Figure 1 E, \* $p < 0.05$ , \*\* $p < 0.01$ ). However, compared to the agomir NC group, the fibrosis degree was significantly lower and  $\alpha$ -SMA and collagen I expression levels were lower in the miR-122-5p agomir group (Figure 1 E, # $p < 0.05$ ). Interestingly, western blot analysis on  $\alpha$ -SMA and collagen I expression corroborated the IHC results; that is,  $\alpha$ -SMA and collagen I levels were stimulated by CAE, and overexpression of miR-122-5p reduced the expression of these two indices (Figure 1 F, \* $p < 0.05$ , # $p < 0.05$ ).

The expression of inflammatory factors (IL-1 $\beta$ , IL-6, and TNF- $\alpha$ ) in serum of AP mice and cells was examined by ELISA. The results showed that the expression levels of IL-1 $\beta$ , IL-6, and TNF- $\alpha$  were significantly higher in the CAE group compared with the vehicle group (Figures 1 G, H, \*\*\* $p < 0.001$ ), which suggested an aggravated inflammatory response, while those cytokines were significantly lower in the miR-122-5p agomir group compared with the agomir NC group (Figures 1 G, H, ### $p < 0.001$ ). Taken together, the above results demonstrated that AP cell and mouse models were successfully created by CAE overstimulation. Moreover, miR-122-5p was lowly expressed in AP mice and cells, and overexpression of miR-122-5p could relieve AP-induced inflammation or fibrosis in mice and cells.

#### miR-122-5p negatively regulated HDAC1

Next, we studied the mechanism of miR-122-5p in reducing the inflammation and fibrosis in AP mice and cells. Jefferson software (<https://cm.jefferson.edu/rna22/Precomputed/>) was used to search for endogenous target genes of miR-

122-5p and found that there was a binding site between miR-122-5p and HDAC1 (Figure 2 A). Hence, we presumed that miR-122-5p may affect AP inflammation and fibrosis via HDAC1. To verify this presumption, HDAC1 expression was measured and the results showed that the CAE group had higher expression of HDAC1 than the vehicle group (Figures 2 B, C, \* $p < 0.05$ ). Dual luciferase reporter gene assay results revealed that, after HDAC1-wt was inserted, the relative luciferase activity in the miR-122-5p agomir group was significantly lower compared with the agomir NC group (Figure 2 D, ## $p < 0.01$ ), while after HDAC1-mut was inserted, there was no significant difference between these two groups (Figure 2 D). This result suggested that HDAC1 was a potential target of miR-122-5p. Afterwards, RNA pull-down results further confirmed the interaction between miR-122-5p and HDAC1 (Figure 2 E, && $p < 0.01$ ). All the results indicated that miR-122-5p may negatively regulate the expression of HDAC1 and thus affect the inflammation and fibrosis in AP.

#### miR-122-5p mitigated the inflammation and fibrosis in AP mice and cells by regulating HDAC1

To further ascertain the impact of miR-122-5p-regulated HDAC1 in AP, we investigated the effects of oe-HDAC1 alone and the synergic effect of miR-122-5p agomir and oe-HDAC1 on inflammation and fibrosis in AP mice and cells. As reflected in qRT-PCR and western blot results, HDAC1 expression in the oe-HDAC1 group or miR-122-5p agomir + oe-HDAC1 group was evidently higher in AP mice and cells when compared with the oe-NC group or miR-122-5p agomir + oe-NC group (Figures 3 A, B, \* $p < 0.05$ , \*\* $p < 0.01$ , & $p < 0.05$ , && $p < 0.01$ ).

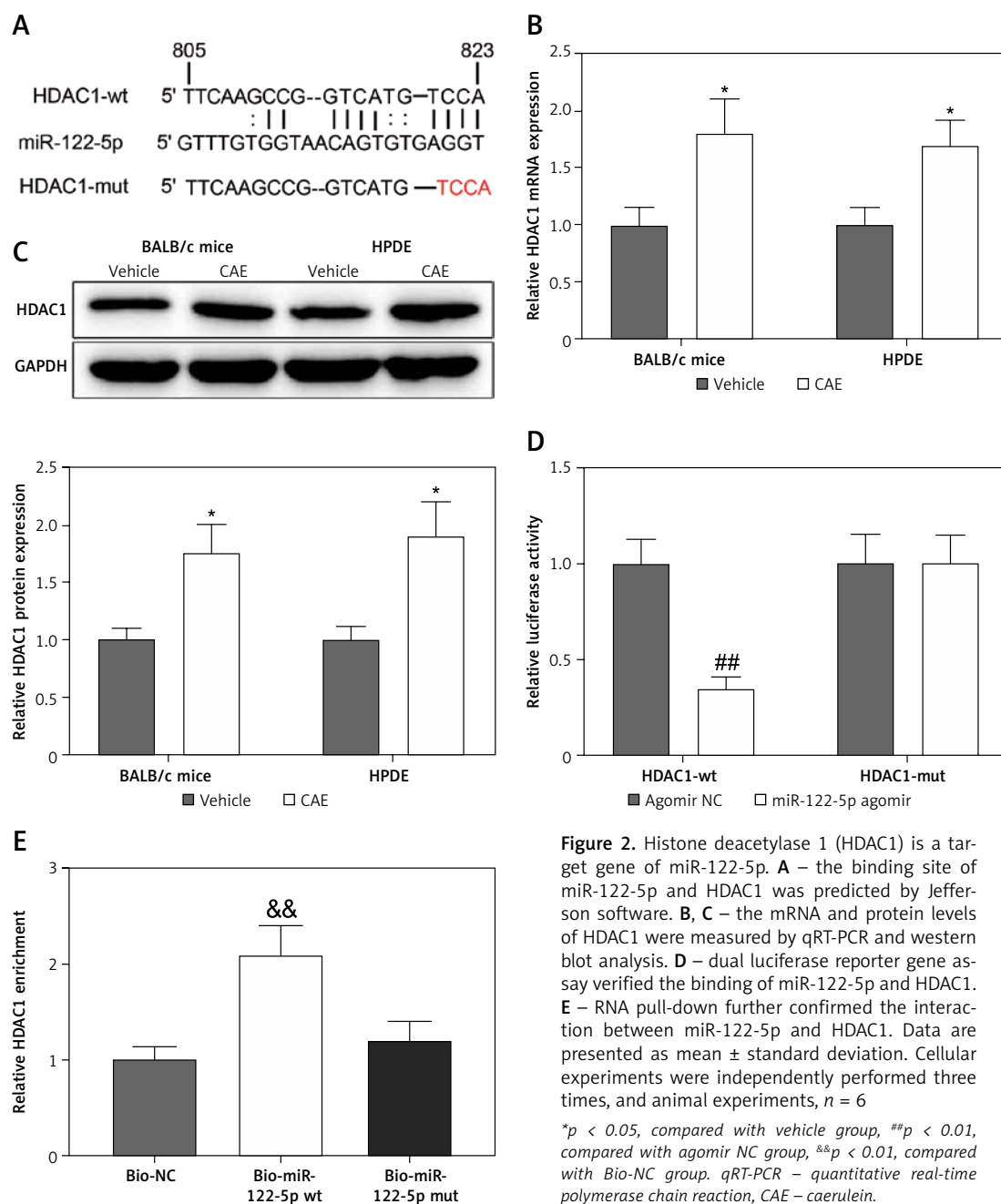
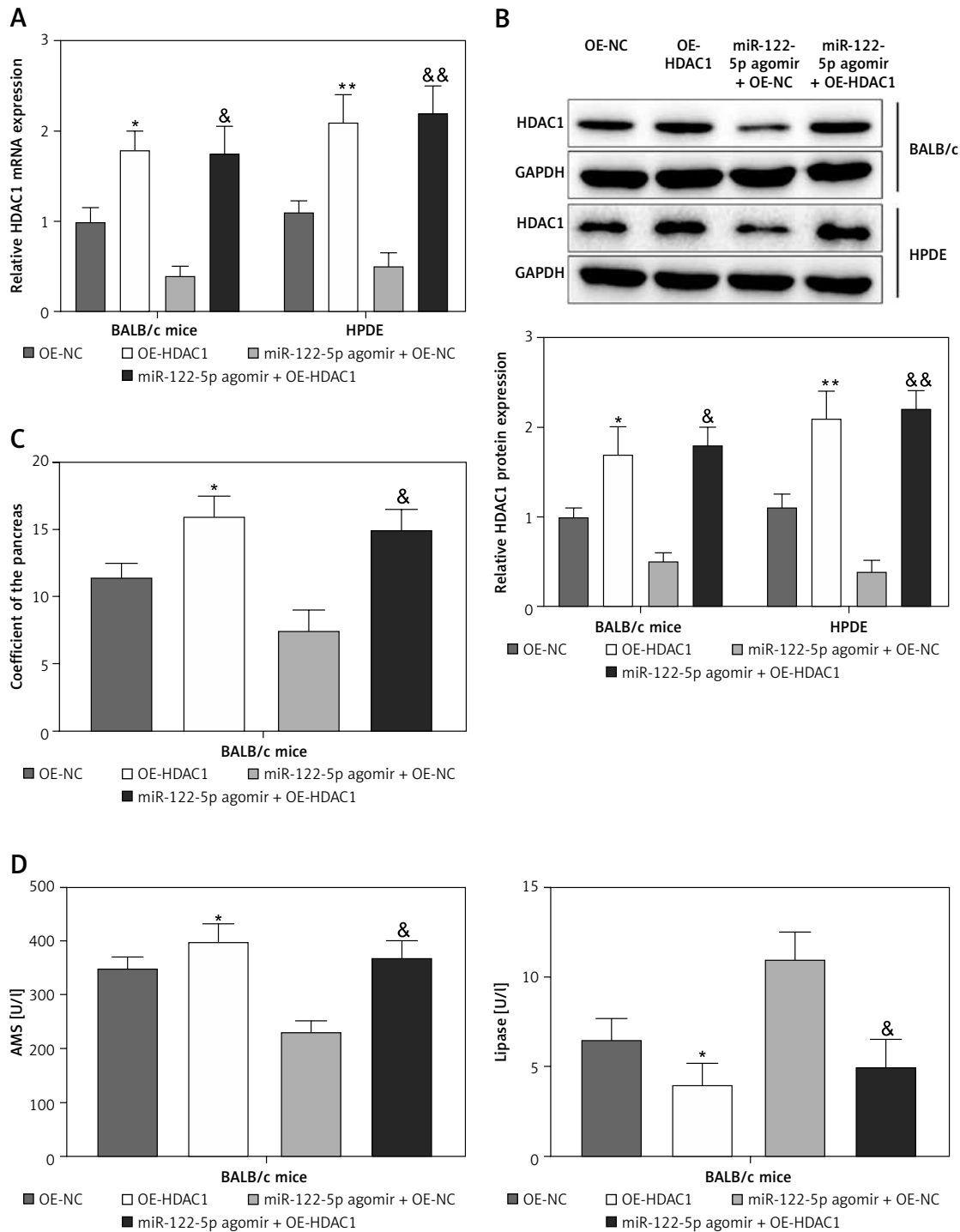


**Figure 2.** Histone deacetylase 1 (HDAC1) is a target gene of miR-122-5p. **A** – the binding site of miR-122-5p and HDAC1 was predicted by Jefferson software. **B, C** – the mRNA and protein levels of HDAC1 were measured by qRT-PCR and western blot analysis. **D** – dual luciferase reporter gene assay verified the binding of miR-122-5p and HDAC1. **E** – RNA pull-down further confirmed the interaction between miR-122-5p and HDAC1. Data are presented as mean  $\pm$  standard deviation. Cellular experiments were independently performed three times, and animal experiments,  $n = 6$

\* $p < 0.05$ , compared with vehicle group, ## $p < 0.01$ , compared with agomir NC group, && $p < 0.01$ , compared with Bio-NC group. qRT-PCR – quantitative real-time polymerase chain reaction, CAE – caerulein.

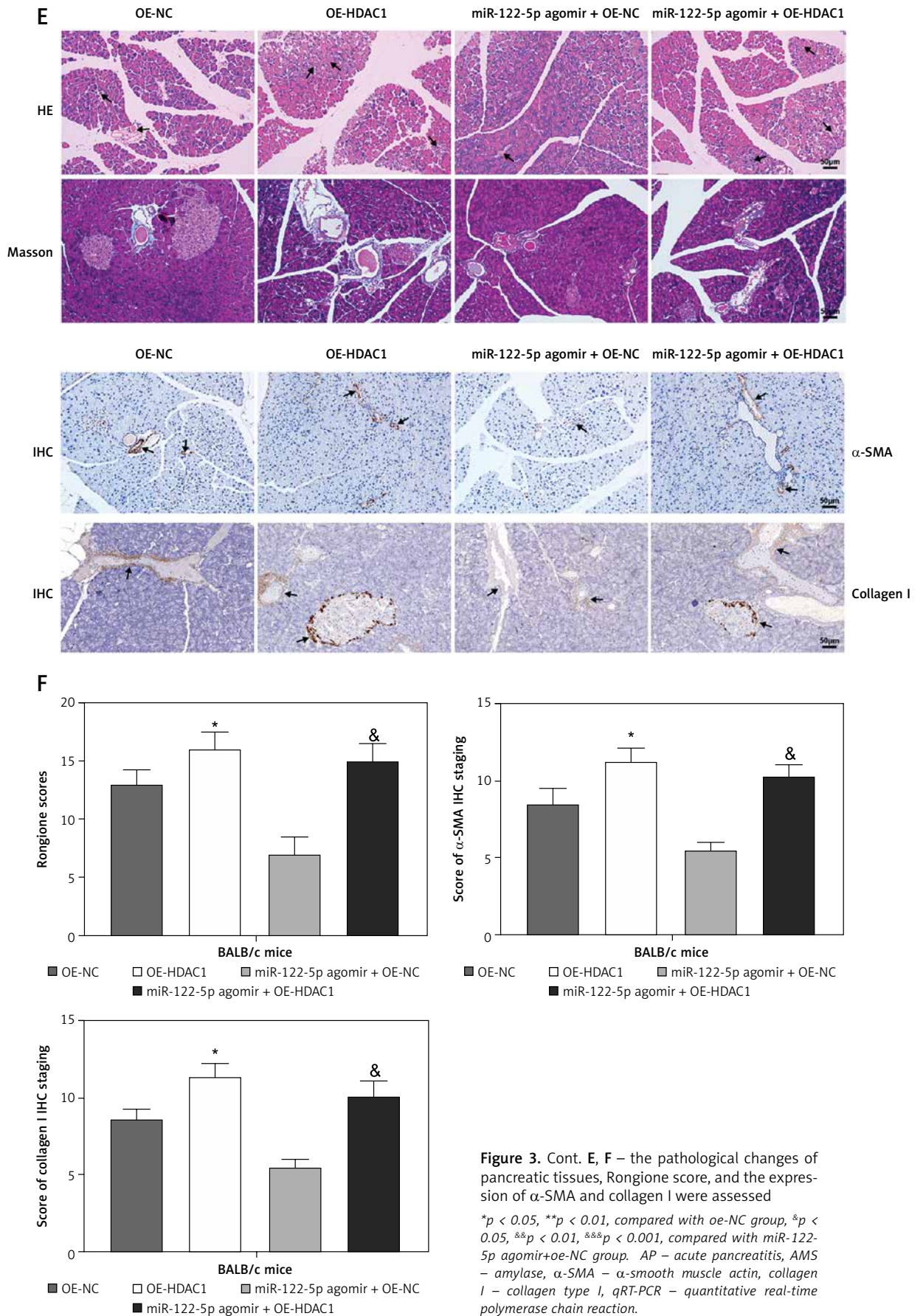
Compared with the oe-NC group or miR-122-5p agomir + oe-NC group, the pancreatic coefficient and AMS expression were increased but the expression of lipase was decreased in the oe-HDAC1 group or miR-122-5p agomir + oe-HDAC1 group (Figures 3 C, D, \* $p < 0.05$ , & $p < 0.05$ ). As shown in Figures 3 E, F, in the oe-HDAC1 group or miR-122-5p agomir + oe-HDAC1 group, the mice had a higher Rongione score, aggravated acinar edema and patellar necrosis, exacerbated pancreatic tissue fibrosis, and enhanced expression of  $\alpha$ -SMA and collagen I (vs. oe-NC group or miR-122-5p agomir + oe-NC group) (\* $p < 0.05$ , & $p < 0.05$ ).

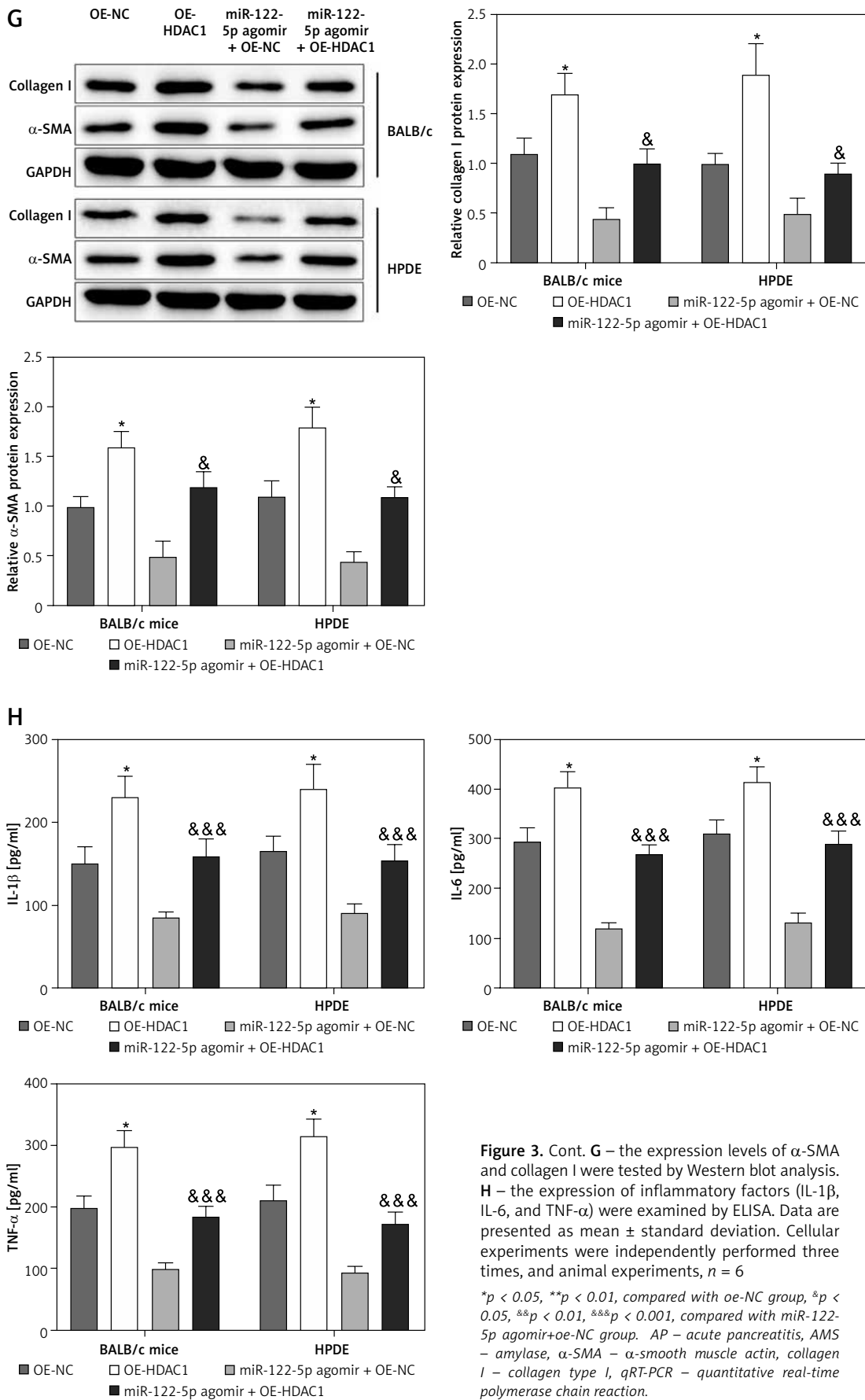
Moreover, the measurement by western blot showed increased  $\alpha$ -SMA and collagen I expression in AP mice and cells in the oe-HDAC1 group and miR-122-5p agomir + oe-HDAC1 group (Figure 3 G, \* $p < 0.05$ , & $p < 0.05$ ). The related inflammatory factors (IL-1 $\beta$ , IL-6, and TNF- $\alpha$ ) in AP mice and cells were detected by ELISA. The results showed that these factors in the oe-HDAC1 group or miR-122-5p agomir + oe-HDAC1 group were markedly increased compared with the oe-NC group or miR-122-5p agomir + oe-NC group (Figure 3 H, \* $p < 0.05$ , && $p < 0.001$ ). These results suggested that miR-122-5p could affect AP-related inflammation and fibrosis through negatively regulating HDAC1.



**Figure 3.** miR-122-5p targets HDAC1 to affect AP mouse and cell inflammation and fibrosis. **A, B** – after cells were transfected with oe-HDAC1 or co-transfected with miR-122-5p agomir and oe-HDAC1, the mRNA and protein expression of HDAC1 was measured by qRT-PCR and western blot. **C, D** – the pancreatic coefficient and the expression of AMS and lipase were evaluated

\* $p < 0.05$ , \*\* $p < 0.01$ , compared with oe-NC group, \* $p < 0.05$ , \*\* $p < 0.01$ , \*\*\* $p < 0.001$ , compared with miR-122-5p agomir+oe-NC group. AP – acute pancreatitis, AMS – amylase,  $\alpha$ -SMA –  $\alpha$ -smooth muscle actin, collagen I – collagen type I, qRT-PCR – quantitative real-time polymerase chain reaction.





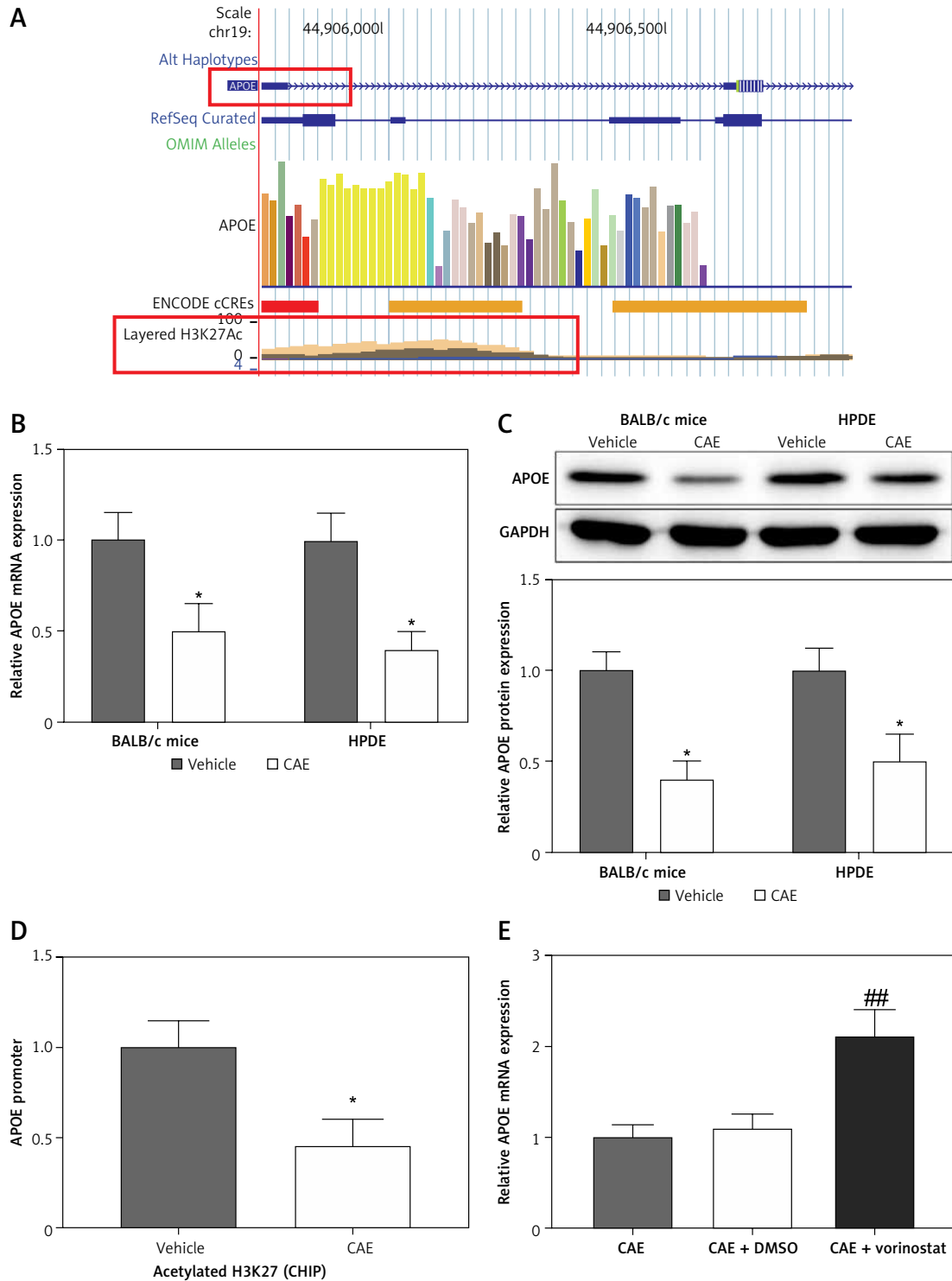


**Figure 4.** Histone deacetylase 1 (HDAC1) facilitates H3 deacetylation and inhibits APOE transcription. **A** – UCSC database analysis showed that H3K27ac was highly enriched in APOE promoter region. **B, C** – the expression of APOE in AP mice and cells was assessed using qRT-PCR and western blot. **D** – the relationship between HDAC1 and APOE was analyzed by ChIP-qPCR assay. **E** – after the pan-HDAC inhibitor vorinostat was added and cultured for 24 h, the mRNA expression of APOE or H3K27ac level was tested by qRT-PCR or ChIP-qPCR

\* $p < 0.05$ , \*\* $p < 0.01$ , \*\*\* $p < 0.001$ , compared with vehicle group, oe-NC group, or oe-HDAC1 (0  $\mu$ g) group, ## $p < 0.01$ , compared with CAE + DMSO group, # $p < 0.05$ , compared with sh-NC group. AP – acute pancreatitis, qRT-PCR – quantitative real-time polymerase chain reaction.

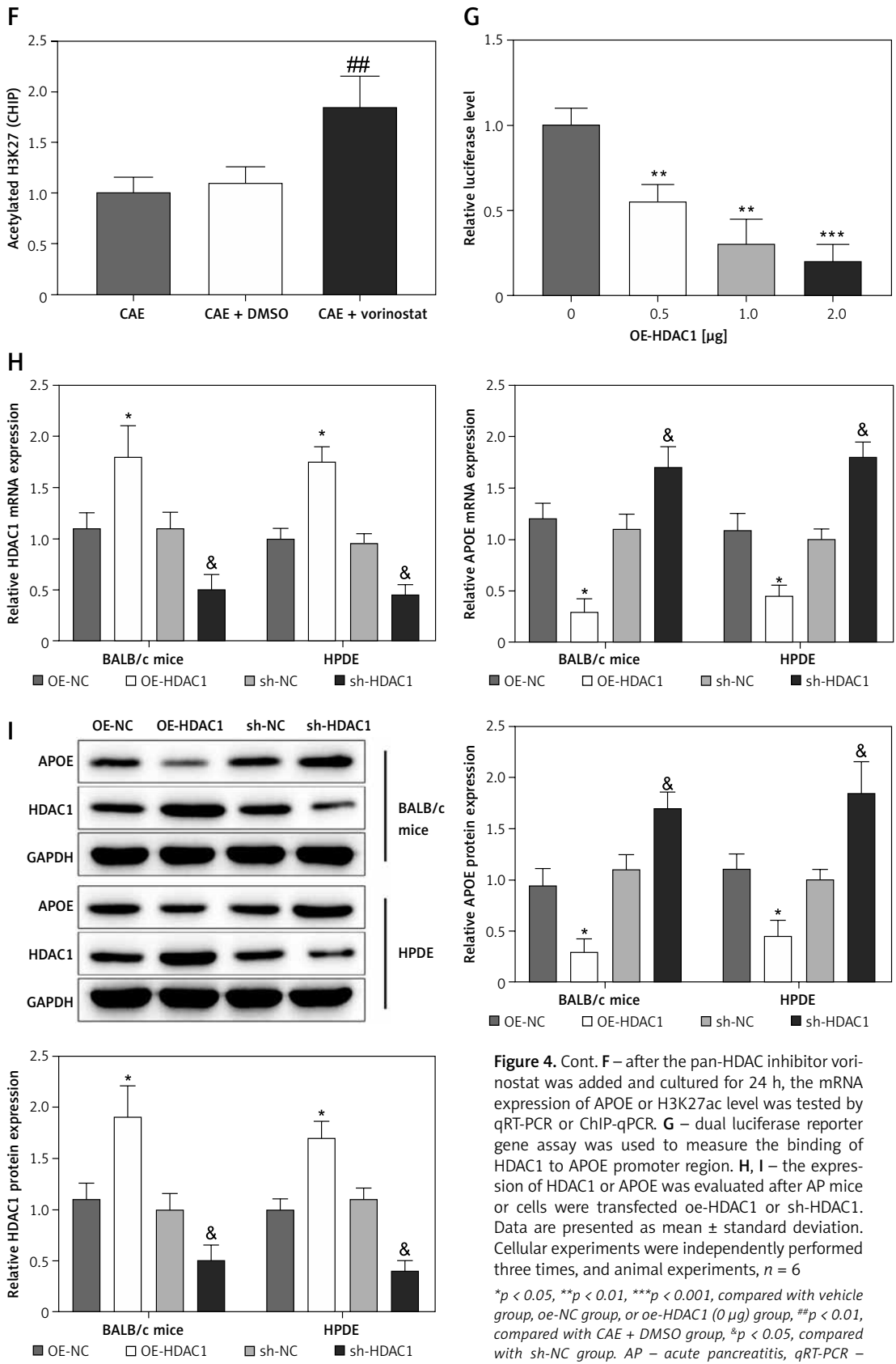


**Figure 4.** Cont. **F** – after the pan-HDAC inhibitor vorinostat was added and cultured for 24 h, the mRNA expression of APOE or H3K27ac level was tested by qRT-PCR or ChIP-qPCR. **G** – dual luciferase reporter gene assay was used to measure the binding of HDAC1 to APOE promoter region. **H, I** – the expression of HDAC1 or APOE was evaluated after AP mice or cells were transfected oe-HDAC1 or sh-HDAC1. Data are presented as mean  $\pm$  standard deviation. Cellular experiments were independently performed three times, and animal experiments,  $n = 6$   
<sup>\*</sup> $p < 0.05$ , <sup>\*\*</sup> $p < 0.01$ , <sup>\*\*\*</sup> $p < 0.001$ , compared with vehicle group, oe-NC group, or oe-HDAC1 (0  $\mu$ g) group, <sup>##</sup> $p < 0.01$ , compared with CAE + DMSO group, <sup>&</sup> $p < 0.05$ , compared with sh-NC group. AP – acute pancreatitis, qRT-PCR – quantitative real-time polymerase chain reaction.

### HDAC1 suppressed APOE transcription by promoting H3 deacetylation

By analyzing the UCSC database, we found that H3K27ac was highly enriched in the APOE promoter region (Figure 4 A), which indicated that APOE expression was regulated by H3 acetylation. In addition, we explored the expression of APOE in AP mice and cells. The results displayed in Figures 4 B, C showed that the CAE-treated mice and cells had much lower APOE expression than the vehicle group ( $*p < 0.05$ ), which revealed that APOE might participate in AP development.

Then, the ChIP-qPCR assay illustrated that the promoter sequence content of APOE was noticeably lower in the CAE group compared with the vehicle group (Figure 4 D,  $*p < 0.05$ ). After the pan-HDAC inhibitor vorinostat (SML0061, Sigma, 0.2  $\mu\text{g}$ ) was added and cultured with CAE-treated cells, the mRNA expression of APOE and the content of APOE promoter were noticeably increased (Figures 4 E, F,  $\#\#p < 0.01$ ). Next, we constructed the pGL3-E-APOE promoter. HEK239T cells were transfected with different concentrations of HDAC1 overexpression plasmids (0, 0.5, 1, and 2  $\mu\text{g}$ ) and transfected with APOE reporter vectors. The luciferase reporter results showed that HDAC1 inhibited the transcriptional activity of APOE promoter in a dose-dependent manner (Figure 4 G,  $**p < 0.01$ ,  $***p < 0.001$ ).

To test whether HDAC1 can regulate APOE expression in AP, we transfected oe-HDAC1 or sh-HDAC1 into AP mice or cells, and then detected APOE expression. Results from qRT-PCR and western blot revealed that oe-HDAC1 observably promoted the expression of HDAC1 in AP mice and cells but observably decreased the expression of APOE; however, opposite results were obtained after transfection with sh-HDAC1 (Figures 4 H, I,  $*p < 0.05$ ,  $\&p < 0.05$ ). It was concluded that HDAC1 promoted H3K27 deacetylation of APOE promoter and inhibited APOE transcription.

### HDAC1 affected AP mouse and cell inflammation and fibrosis by regulating APOE

To further investigate the effect of HDAC1 and APOE on inflammation and fibrosis in AP mice and cells, we injected or transfected oe-APOE, oe-APOE + oe-HDAC1, or their corresponding controls, into AP mice or cells. APOE expression in oe-APOE or oe-APOE + oe-HDAC1 group was conspicuously higher compared with the oe-NC or oe-HDAC1 + oe-NC group (Figures 5 A, B,  $*p < 0.05$ ,  $**p < 0.01$ ,  $\&p < 0.05$ ).

Next, we deeply researched their effect on the inflammation and fibrosis in AP mice or cells through a series of experiments. In the oe-APOE

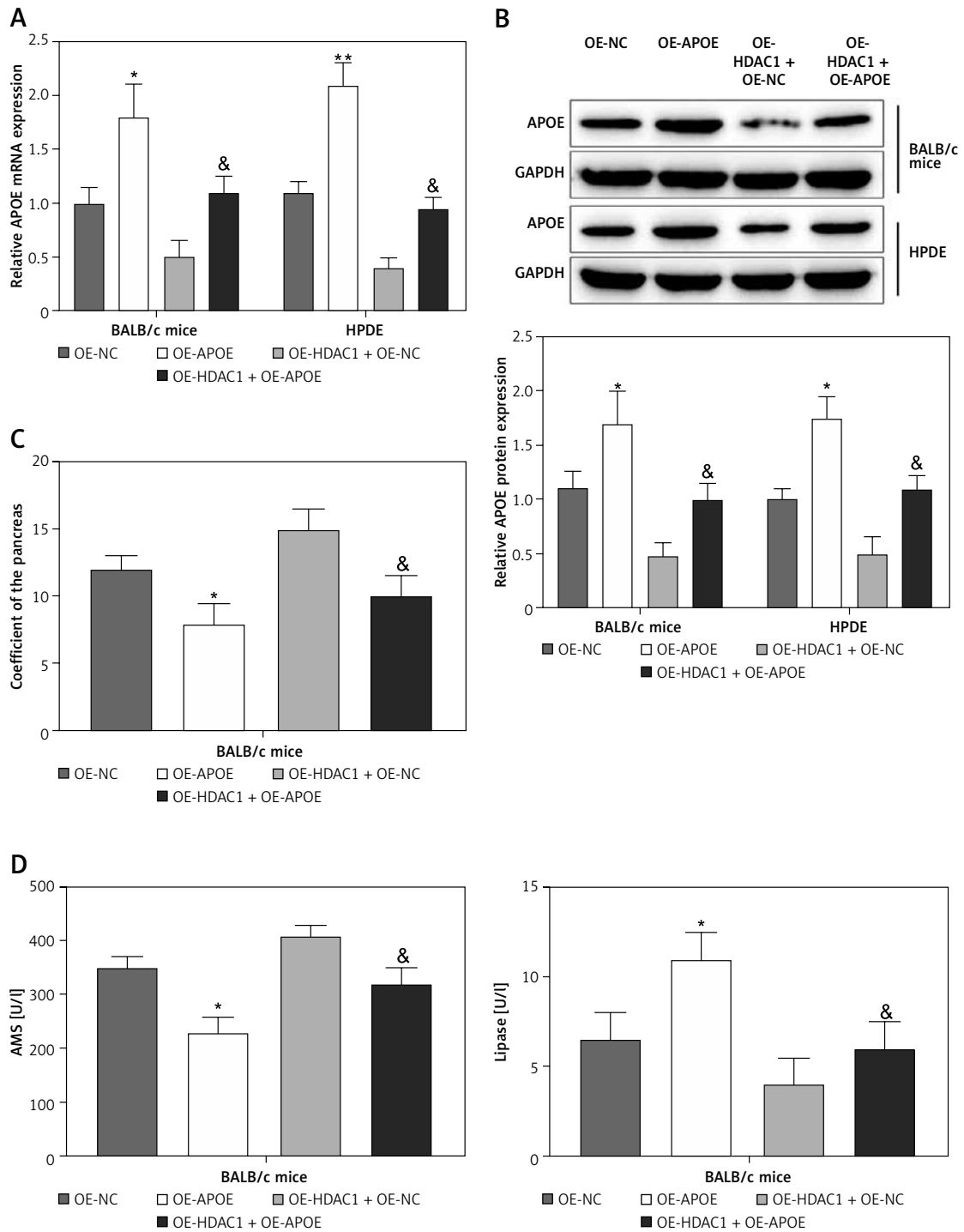
or oe-APOE + oe-HDAC1 group, remarkable reductions of the pancreatic coefficient and AMS expression and enhancement of lipase expression were noted in AP mice, compared with their corresponding control groups (Figures 5 C, D,  $*p < 0.05$ ,  $\&p < 0.05$ ). In contrast to the oe-NC or oe-HDAC1 + oe-NC group, the Rongione score was considerably decreased, and acinar edema and patchy necrosis evidently relieved, in the oe-APOE or oe-APOE + oe-HDAC1 group; the degree of fibrosis was remarkably perturbed, and  $\alpha$ -SMA and collagen I expression prominently decreased, in the oe-APOE or oe-APOE + oe-HDAC1 group (Figures 5 E, F,  $*p < 0.05$ ,  $\&p < 0.05$ ). As expected, western blot for detection of protein expression of  $\alpha$ -SMA and collagen I showed that the oe-APOE or oe-APOE + oe-HDAC1 group had lower  $\alpha$ -SMA and collagen I versus the oe-NC or oe-HDAC1 + oe-NC group (Figure 5 G,  $*p < 0.05$ ,  $\&p < 0.05$ ). In ELISA, the expression levels of IL-1 $\beta$ , IL-6, and TNF- $\alpha$  in AP mice and cells were dramatically diminished in the oe-APOE or oe-APOE + oe-HDAC1 group (Figure 5 H,  $***p < 0.001$ ,  $\&p < 0.05$ ). In conclusion, these results suggested that HDAC1 may affect inflammation and fibrosis in AP mice or cells by activating APOE expression.

### miR-122-5p attenuated the inflammation and fibrosis in AP mice or cells by suppressing HDAC1-mediated inhibition of APOE

In the above experiments, we found that miR-122-5p could regulate HDAC1, and HDAC1 could promote H3 deacetylation and inhibit APOE transcription, thus affecting inflammation or fibrosis in AP mice and cells. Therefore, we hypothesized that miR-122-5p might downregulate HDAC1 and promote APOE transcription, thereby reducing inflammation or fibrosis in AP mice and cells. To confirm our hypothesis, we transfected miR-122-5p agomir + sh-NC, miR-122-5p agomir + sh-APOE, and the corresponding controls into AP cells and mice, and observed their effect on inflammation or fibrosis in AP cells and mice.

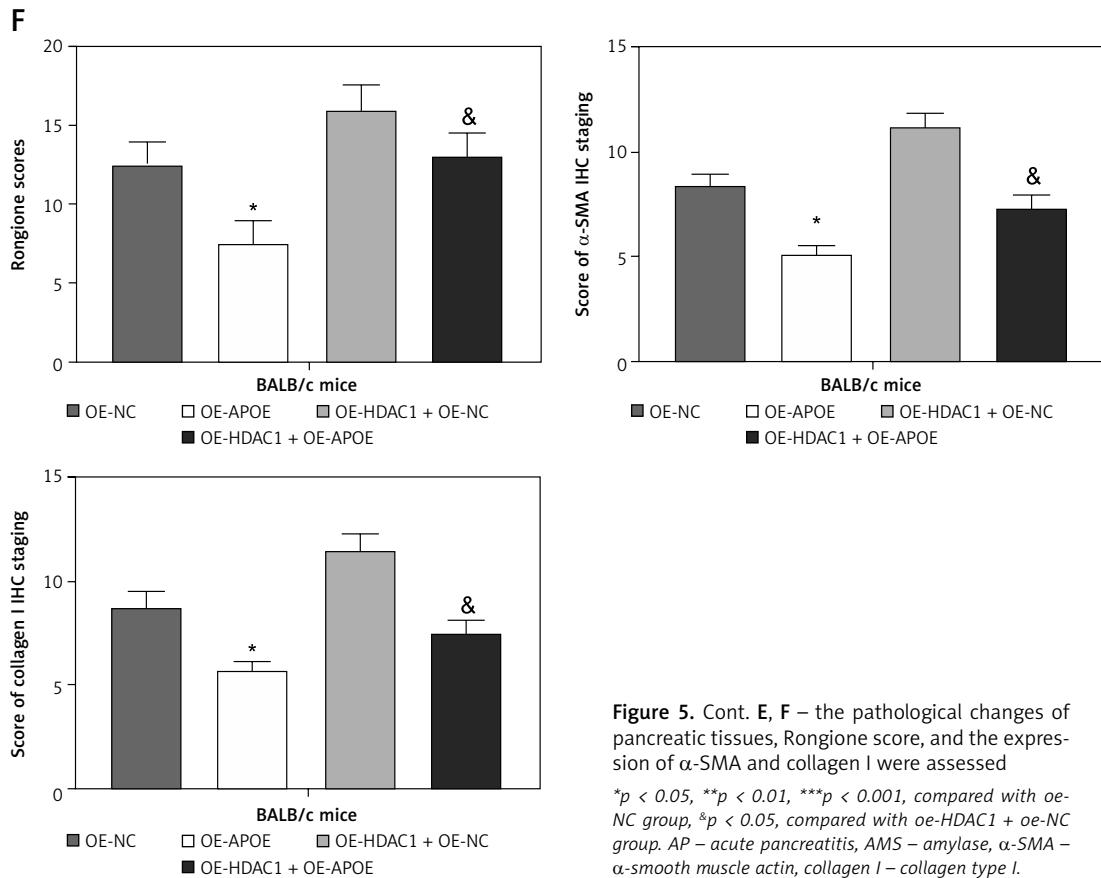
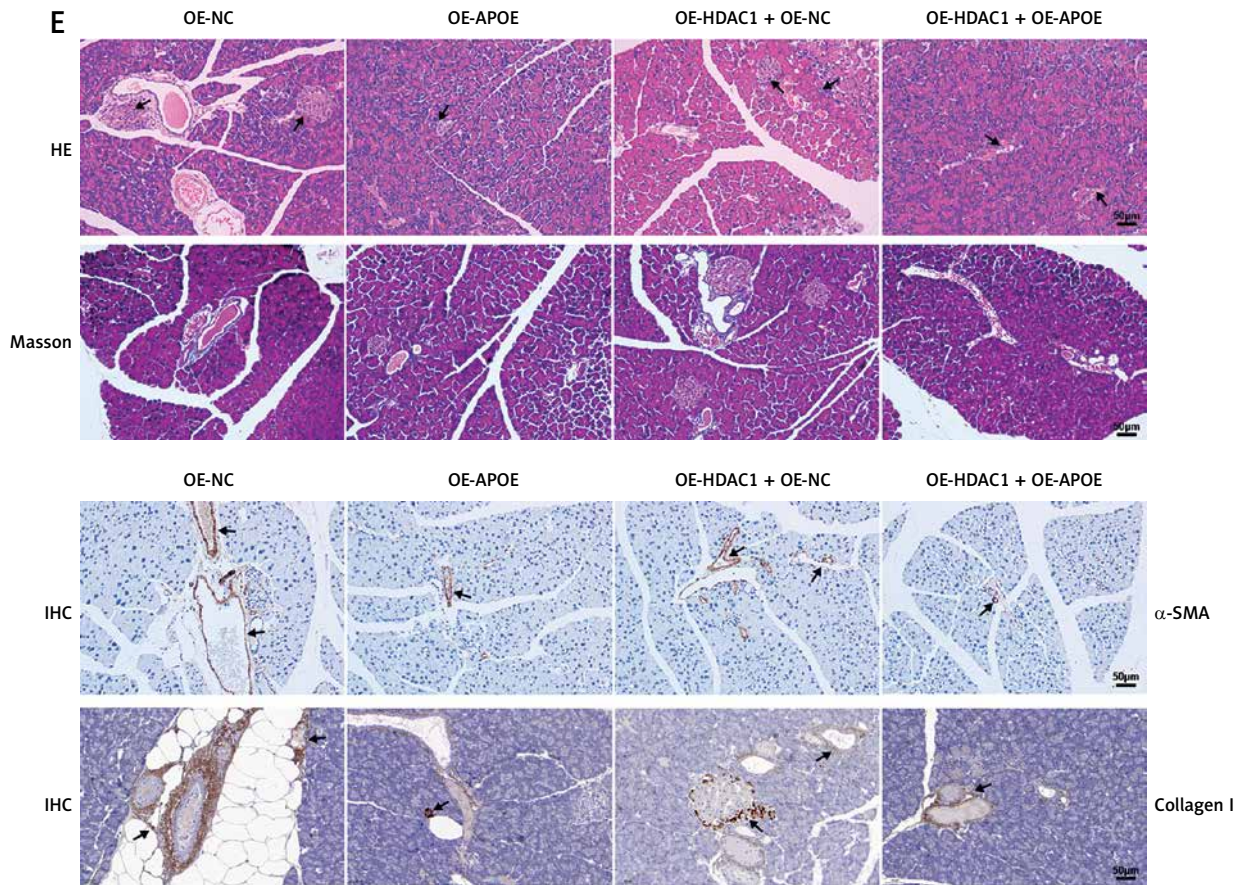
First, the expression levels of HDAC1 and APOE were measured and the results showed that HDAC1 expression was significantly lower but APOE expression was significantly higher in the miR-122-5p agomir + sh-NC group (vs agomir-NC + sh-NC group), while in the miR-122-5p agomir + sh-APOE group, HDAC1 expression was not significantly different and APOE expression was significantly lower, compared with the miR-122-5p agomir + sh-NC group (Figures 6 A–C,  $*p < 0.05$ ,  $**p < 0.01$ ,  $\&p < 0.05$ ).

Compared with the miR-122-5p agomir + sh-NC group, the pancreatic coefficient and the expression of AMS were increased but lipase ex-



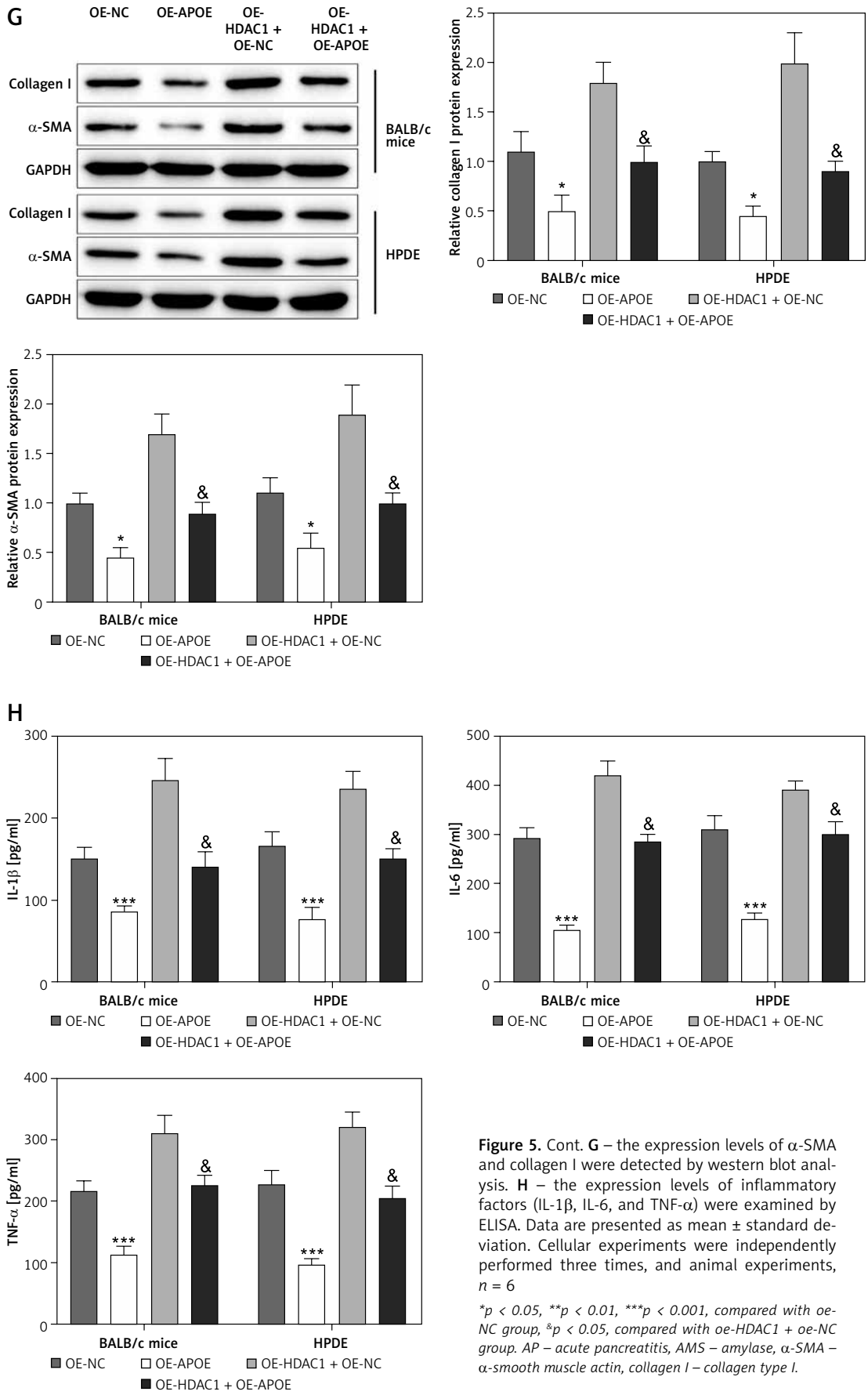
**Figure 5.** Histone deacetylase 1 (HDAC1) affects inflammation and fibrosis in AP mice or cells by activating APOE. **A, B** – after AP mice or cells were transfected with oe-APOE or oe-APOE + oe-HDAC1 respectively, APOE expression was measured by qRT-PCR and western blot. **C, D** – the pancreatic coefficient and the expression of AMS and lipase were evaluated

\* $p < 0.05$ , \*\* $p < 0.01$ , \*\*\* $p < 0.001$ , compared with oe-NC group, & $p < 0.05$ , compared with oe-HDAC1 + oe-NC group. AP – acute pancreatitis, AMS – amylase,  $\alpha$ -SMA –  $\alpha$ -smooth muscle actin, collagen I – collagen type I.



**Figure 5.** Cont. E, F – the pathological changes of pancreatic tissues, Rongione score, and the expression of  $\alpha$ -SMA and collagen I were assessed

\* $p < 0.05$ , \*\* $p < 0.01$ , \*\*\* $p < 0.001$ , compared with oe-NC group, & $p < 0.05$ , compared with oe-HDAC1 + oe-NC group. AP – acute pancreatitis, AMS – amylase,  $\alpha$ -SMA –  $\alpha$ -smooth muscle actin, collagen I – collagen type I.



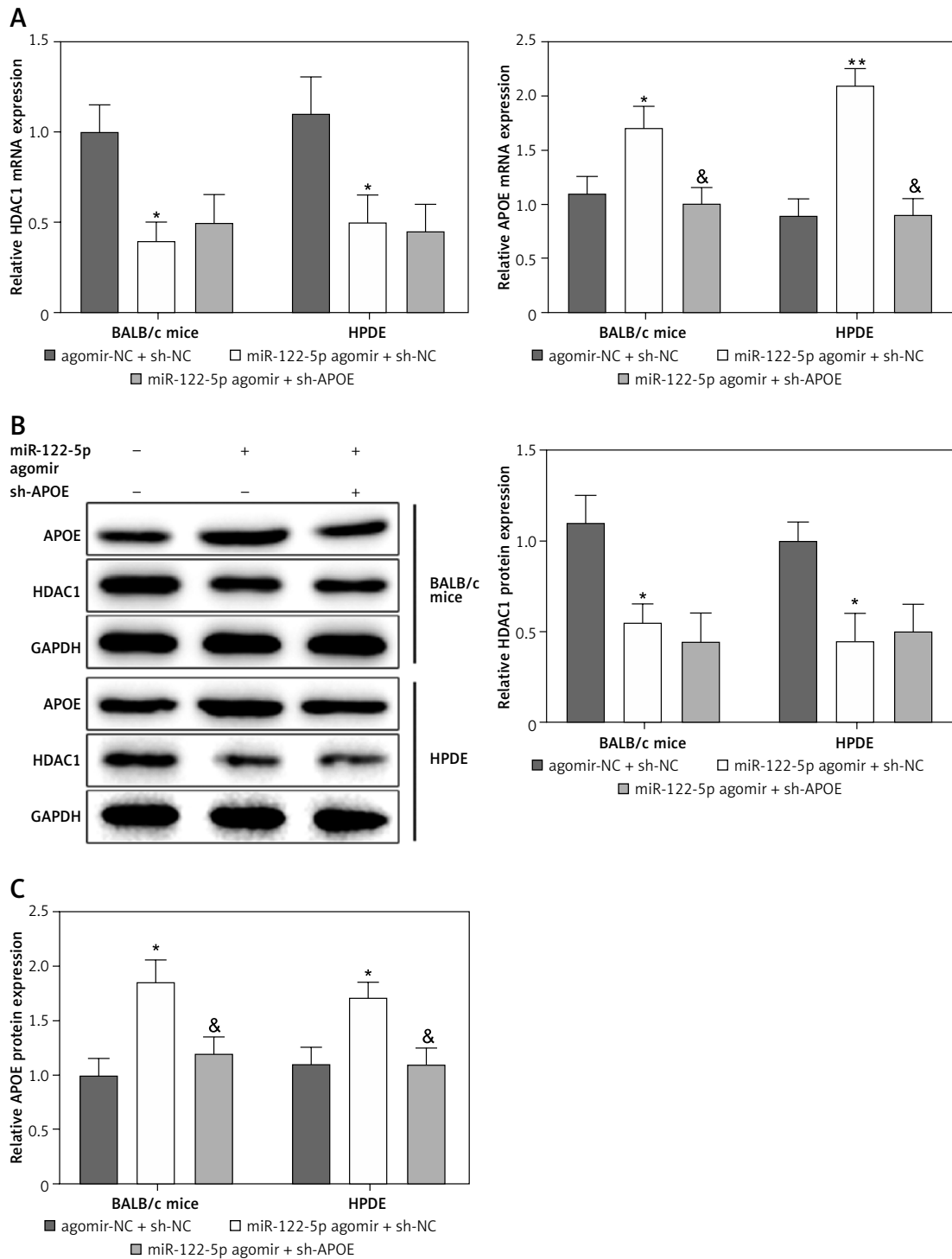


**Figure 6.** miR-122-5p alleviates inflammation and fibrosis in AP mice or cells by binding HDAC1 to promote APOE transcription. **A, B** – the mRNA and protein levels of HDAC1 and APOE were measured. **C** – the pancreatic coefficient and the expression of AMS and lipase were evaluated

\* $p < 0.05$ , \*\* $p < 0.01$ , \*\*\* $p < 0.001$ , compared with agomir-NC + sh-NC group, & $p < 0.05$ , && $p < 0.001$ , compared with miR-122-5p agomir + sh-NC group. AP – acute pancreatitis, AMS – amylase,  $\alpha$ -SMA –  $\alpha$ -smooth muscle actin, collagen I – collagen type I.

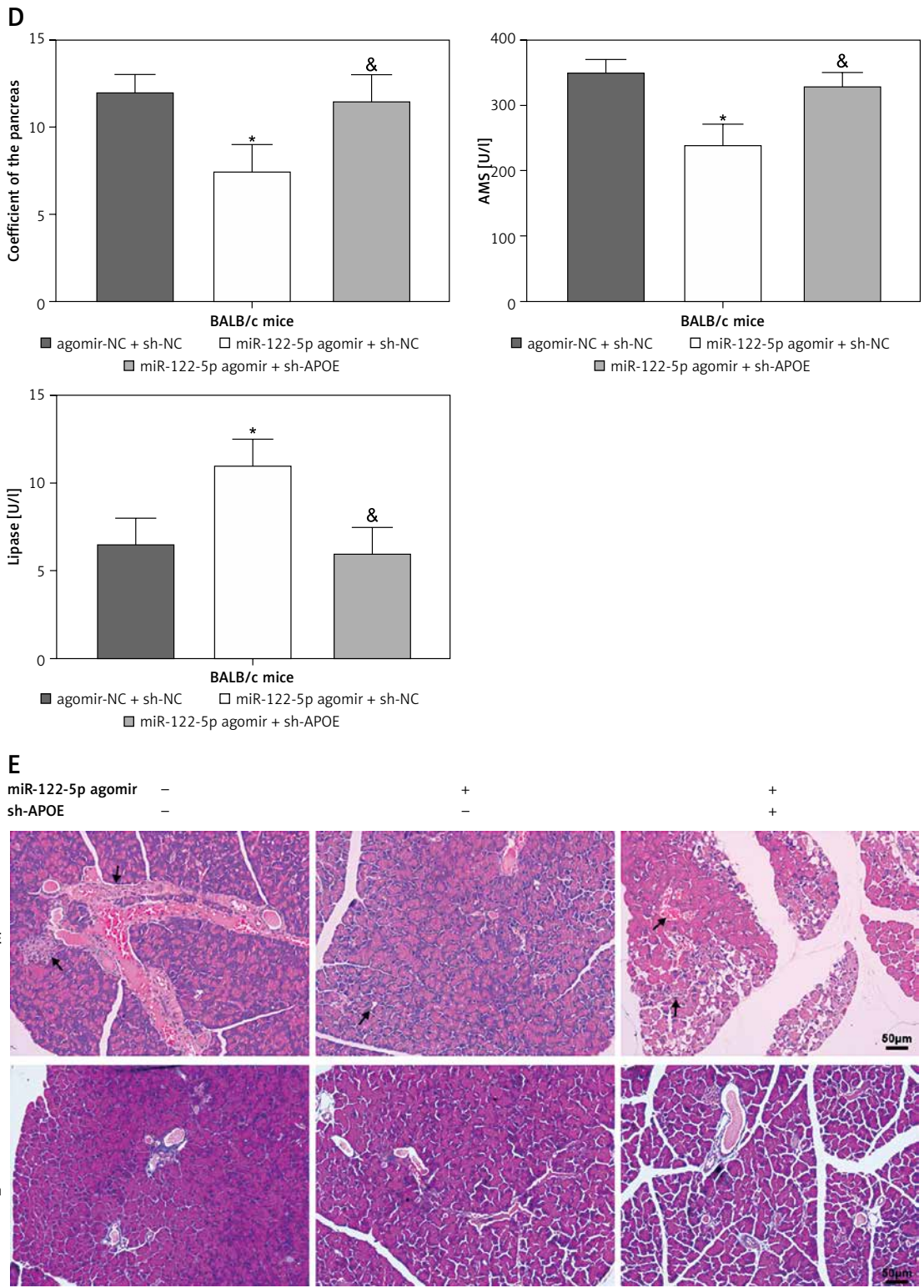


**Figure 6.** Cont. **D** – the pancreatic coefficient and the expression of AMS and lipase were evaluated. **E** – the pathological changes of pancreatic tissues, Rongione score, and the expression of  $\alpha$ -SMA and collagen I were evaluated \* $p < 0.05$ , \*\* $p < 0.01$ , \*\*\* $p < 0.001$ , compared with agomir-NC + sh-NC group, & $p < 0.05$ , && $p < 0.001$ , compared with miR-122-5p agomir + sh-NC group. AP – acute pancreatitis, AMS – amylase,  $\alpha$ -SMA –  $\alpha$ -smooth muscle actin, collagen I – collagen type I.

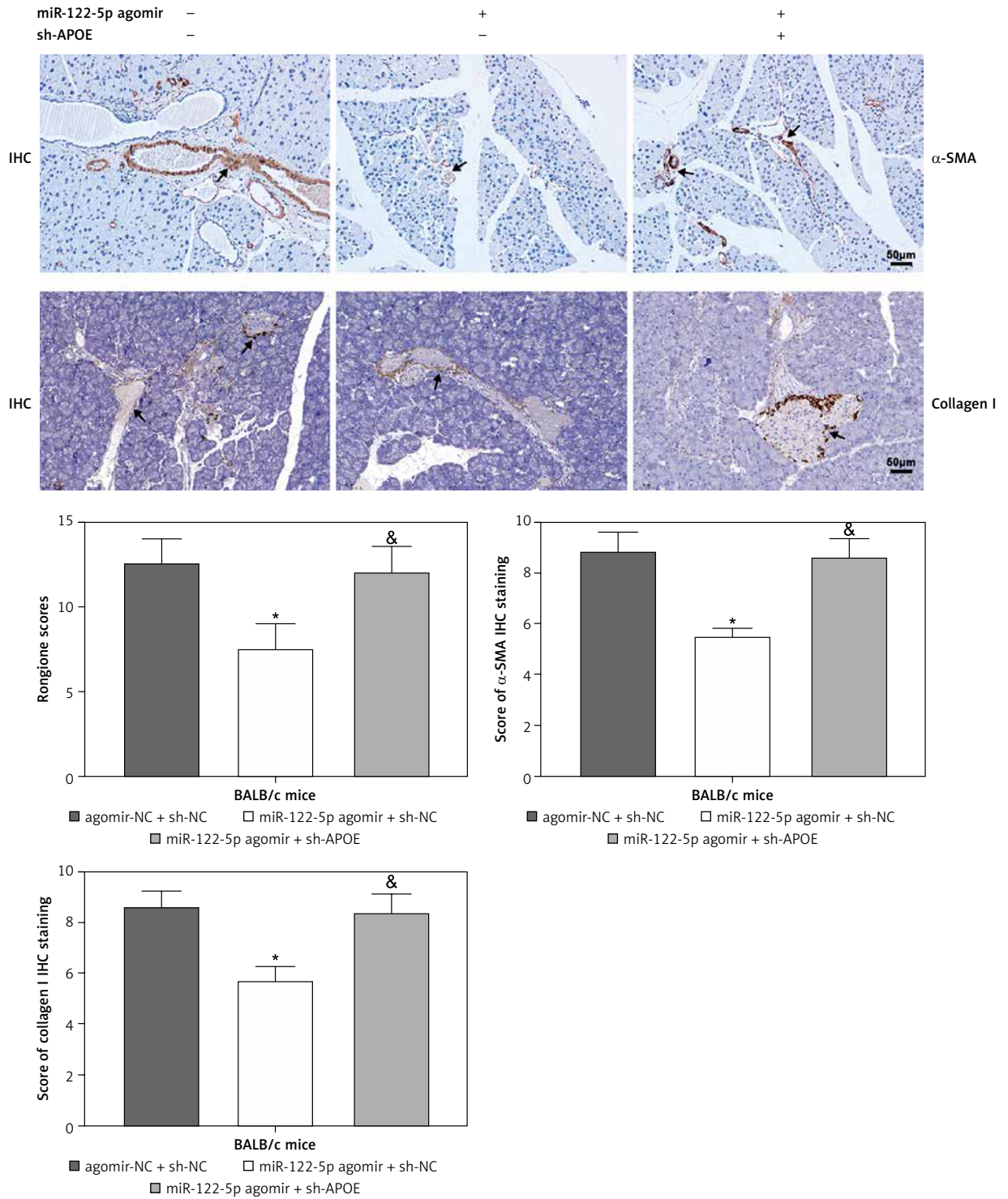
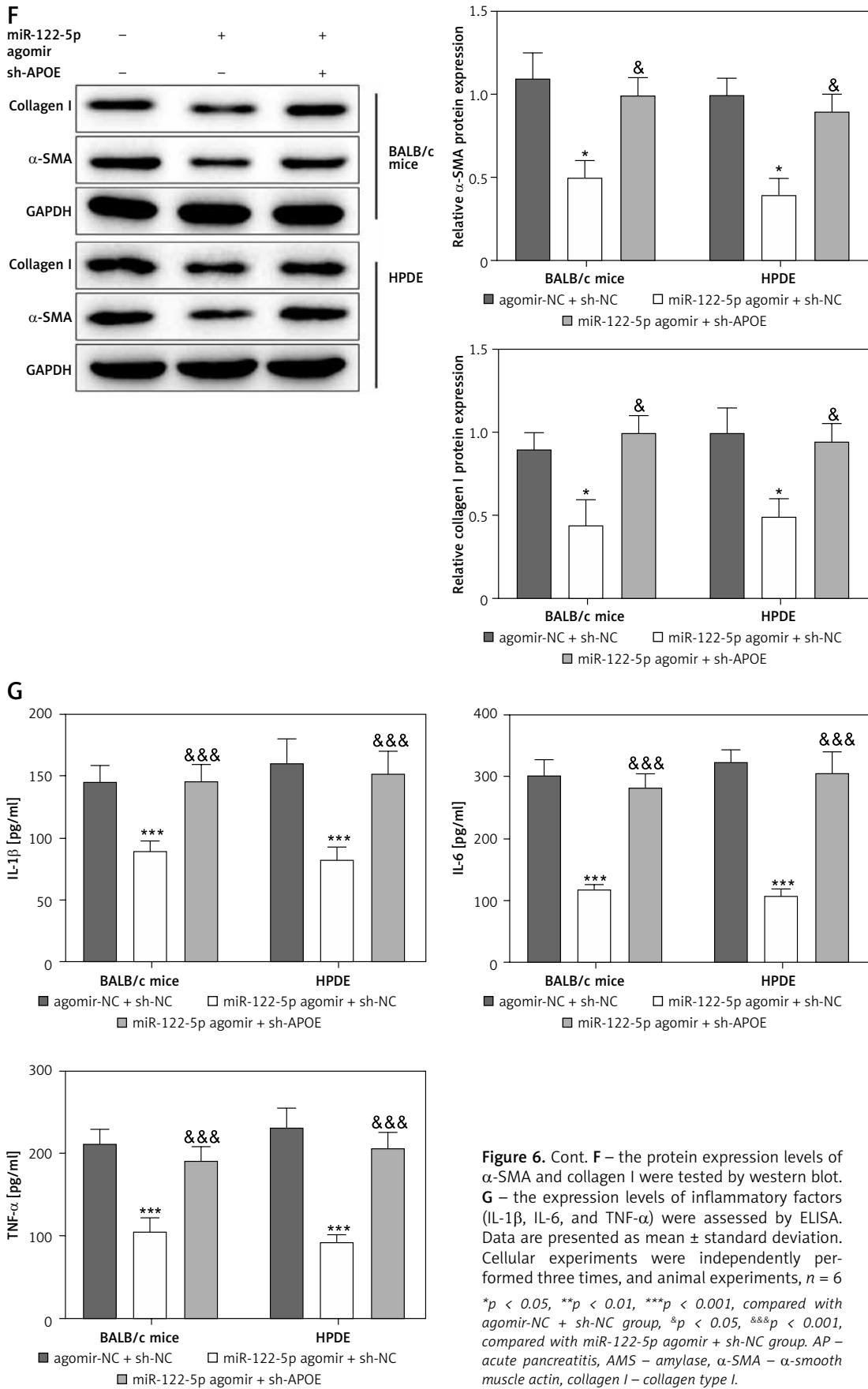


**Figure 6.** Cont. **E** – the pathological changes of pancreatic tissues, Rongione score, and the expression of  $\alpha$ -SMA and collagen I were evaluated

\* $p < 0.05$ , \*\* $p < 0.01$ , \*\*\* $p < 0.001$ , compared with agomir-NC + sh-NC group, & $p < 0.05$ , && $p < 0.001$ , compared with miR-122-5p agomir + sh-NC group. AP – acute pancreatitis, AMS – amylase,  $\alpha$ -SMA –  $\alpha$ -smooth muscle actin, collagen I – collagen type I.



pression was repressed in the miR-122-5p agomir + sh-APOE group (Figure 6 D,  $*p < 0.05$ ). Results from H&E, Masson, and IHC staining revealed that the miR-122-5p agomir + sh-APOE group exhibited an increased Rongione score, accentuated acinar edema and patchy necrosis, accelerated degree of fibrosis, and elevated  $\alpha$ -SMA and collagen I expression (Figure 6 E,  $*p < 0.05$ ). The results of western blot analysis showed that  $\alpha$ -SMA and collagen I expression in mice and cells were prominently increased in the miR-122-5p agomir + sh-APOE group (Figure 6 F,  $*p < 0.05$ ). ELISA results showed that the expression of inflammatory factors (IL-1 $\beta$ , IL-6, and TNF- $\alpha$ ) was dramatically increased in mice and cells from the miR-122-5p agomir + sh-APOE group (Figure 6 G,  $***p < 0.001$ ).

In summary, miR-122-5p alleviated inflammation and fibrosis in AP mice or cells by binding HDAC1 to promote APOE transcription.

## Discussion

Acute pancreatitis is an inflammatory disease of the pancreas, which is the main cause of gastrointestinal hospitalizations in many countries [20]. In the United States, AP is a major financial burden, especially in severe cases [21]. However, the pathogenesis of AP is still unclear, highlighting the inevitability and necessity of investigations on the regulatory mechanisms behind AP initiation and development. Inflammation can lead to tissue fibrosis, which, in turn, results in lasting and irreversible damage to organ function [22]. This study focused on the mechanisms of miR-122-5p affecting the inflammatory response and fibrosis in AP using cellular and animal experiments. Our findings revealed that overexpression of miR-122-5p ameliorated inflammation and fibrosis in AP mice or cells by binding HDAC1 and promoting APOE transcription.

Previously, miR-122-5p has been linked with inflammation and pancreatitis. A recent study showed that miR-122-5p could interact with the lncRNA XIST to regulate the inflammation and apoptosis in acute kidney injury [23]. In CP, miR-122-5p was found to be underexpressed [24]. In our study, we first found miR-122-5p was decreasingly expressed in AP mice and cells, and the inflammation and fibrosis in AP mice were significantly blunted after miR-122-5p was overexpressed. When it comes to the mechanisms of action of miRs, the miR-mRNA regulatory modules are commonly investigated by researchers. Previously, miR-135b-5p was verified to target HDAC1 and facilitate inflammation in human umbilical vein endothelial cells [25]. miR-125a was also observed to suppress fibrosis in a mouse model of diabetic nephropathy directly by binding to HDAC1 and HDAC1 overexpression reversed the anti-

fibrotic effects of miR-125a [26]. By reviewing the published studies, miR-122-5p was identified to be lowly expressed and targeted the transforming growth factor- $\beta$  receptor-II to affect the progression of skeletal muscle fibrosis [27] and served as a liver-specific miR in chronic hepatitis E [28]. Moreover, HDAC1 was increasingly expressed in myocardial fibrosis [13] and promoted the progression of renal fibrosis [12]. Herein, we found a binding site between miR-122-5p and HDAC1 using a bioinformatics tool. HDAC1 was found to be highly expressed, and upregulated HDAC1 exacerbated AP-induced inflammation and fibrosis. Our data displayed that HDAC1 played a pro-inflammatory and pro-fibrotic role in AP. As expected, HDAC1 overexpression counteracted the anti-inflammatory and anti-fibrosis effects of miR-122-5p in CAE-induced AP mouse and cell models.

Reportedly, HDAC modulated trypsin activation, inflammation, and tissue damage in AP, and HDAC inhibition exerted protective effects in AP [29]. HDAC1 is an important epigenetic protein, which can antagonize the acetylation of histones and non-histone proteins [30]. A recent study demonstrated that ATF4-mediated HDAC1 promoted the progression (including cell proliferation, apoptosis, and inflammation) of AP [31]. Moreover, studies showed that HDAC1 was elevated in lung carcinoma [32], and involved in cancer associated fibroblast activation in lung cancer [33]. The reduction of HDACs' expression may interfere with proper MICEE function and be crucial for idiopathic pulmonary fibrosis [34]. Our results add to the literature indicating that overexpression HDAC1 could aggravate the degree of inflammation and fibrosis in AP mice or cells. HDAC1 has been shown to play a key role in regulating eukaryotic gene expression as a histone deacetylase [13]. For example, butyrate blocked NLR family pyrin domain-containing 3 inflammasome and immune cell infiltration by repressing interactions between HDAC1 and activator protein 1 and STAT1 with increased histone acetylation at H3K9, H3K14, H3K18, and H3K27 loci in AP [35]. H3K27ac enrichment was reported in the promoter region of APOE by the UCSC database, suggesting the regulation of APOE expression by H3 acetylation. APOE was reported to be beneficial to the resolution of pulmonary fibrosis [36]. In the present study, we first demonstrated the targeting relationship between APOE and HDAC1 by ChIP assay, and then concluded that HDAC1 promoted H3K27 deacetylation in the APOE promoter and inhibited APOE transcription. Additionally, APOE was decreased in AP mice and cells and overexpression of APOE could reduce inflammation and fibrosis in AP. However, upregulated HDAC1 could inhibit the anti-inflammatory and anti-fibrosis effects of APOE overexpression.

Rescue experiments revealed that inhibition of APOE suppressed the anti-inflammatory and anti-fibrotic effects of miR-122-5p overexpression. These results suggest that miR-122-5p could reduce inflammation and fibrosis in AP cells and mice by downregulating HDAC1 to promote APOE transcription. More importantly, previous findings showed that APOE was primarily expressed in three isoforms, namely, APOE2, APOE3, and APOE4 [37]. APOE2 and APOE4 were reported to be critically associated with the hyperlipidemia process [38]. Moreover, Du S et al. reported that APOE2 was highly expressed in pancreatic cancer tissues, and promoted pancreatic cancer cell proliferation via regulation of the c-Myc-p21<sup>Waf1</sup> signaling pathway [39]. APOE4 is considered a risk factor for Alzheimer's disease and neurodegeneration, which were deeply involved with inflammation [40, 41]. In our paper, we only studied the regulation of APOE gene expression. Therefore, exploring which isoforms of APOE play a role in AP may be an interesting research topic for our further study.

In conclusion, this study proposed a novel axis, miR-122-5p/HDAC1/APOE, relating to inflammation in AP. These findings, therefore, highlight the potential of these genes as therapeutic targets for AP. However, since miRs exert promiscuous actions and expression of the protein in question may be regulated by multiple miRs, the current study cannot exclude the possibility that miR-122-5p and HDAC1 regulate other downstream genes in AP. Therefore, exploring the regulatory network of miR-122-5p in AP may contribute to its pre-clinical application.

### Acknowledgments

This research was funded by the National Natural Science Foundation of China (No. 82170061) and the Natural Science Foundation of Hunan Province (No. 2022JJ40836).

### Conflict of interest

The authors declare no conflict of interest.

### References

- Petrov MS, Yadav D. Global epidemiology and holistic prevention of pancreatitis. *Nat Rev Gastroenterol Hepatol* 2019; 16: 175-84.
- Leppaniemi A, Tolonen M, Tarasconi A, et al. 2019 WSES guidelines for the management of severe acute pancreatitis. *World J Emerg Surg* 2019; 14: 27.
- Silva-Vaz P, Abrantes AM, Castelo-Branco M, et al. Multifactorial scores and biomarkers of prognosis of acute pancreatitis: applications to research and practice. *Int J Mol Sci* 2020; 21: 338.
- Peng C, Li Z, Yu X. The role of pancreatic infiltrating innate immune cells in acute pancreatitis. *Int J Med Sci* 2021; 18: 534-45.
- Lu TX, Rothenberg ME. MicroRNA. *J Allergy Clin Immunol* 2018; 141: 1202-7.
- Cui J, Zhou B, Ross SA, Zempleni J. Nutrition, microRNAs, and human health. *Adv Nutr* 2017; 8: 105-12.
- Khan IA, Rashid S, Singh N, et al. Panel of serum miRNAs as potential non-invasive biomarkers for pancreatic ductal adenocarcinoma. *Sci Rep* 2021; 11: 2824.
- Dai C, Zhang Y, Xu Z, Jin M. MicroRNA-122-5p inhibits cell proliferation, migration and invasion by targeting CCNG1 in pancreatic ductal adenocarcinoma. *Cancer Cell Int* 2020; 20: 98.
- Wang TZ, Lin DD, Jin BX, Sun XY, Li N. Plasma microRNA: a novel non-invasive biomarker for HBV-associated liver fibrosis staging. *Exp Ther Med* 2019; 17: 1919-29.
- Zhu Z, Xu X, Wang F, et al. Integrative microRNA and mRNA expression profiling in acute aristolochic acid nephropathy in mice. *Mol Med Rep* 2020; 22: 3367-77.
- Kim MY, Yan B, Huang S, Qiu Y. Regulating the regulators: the role of histone deacetylase 1 (HDAC1) in erythropoiesis. *Int J Mol Sci* 2020; 21: 8460.
- Lai L, Cheng P, Yan M, Gu Y, Xue J. Aldosterone induces renal fibrosis by promoting HDAC1 expression, deacetylating H3K9 and inhibiting klotho transcription. *Mol Med Rep* 2019; 19: 1803-8.
- Deng M, Yang S, Ji Y, et al. Overexpression of peptidase inhibitor 16 attenuates angiotensin II-induced cardiac fibrosis via regulating HDAC1 of cardiac fibroblasts. *J Cell Mol Med* 2020; 24: 5249-59.
- Nowak JK, Szczepanik M, Wojsyk-Banaszak I, et al. Cystic fibrosis dyslipidaemia: a cross-sectional study. *J Cyst Fibros* 2019; 18: 566-71.
- Stokman G, van den Hoek AM, Denker Thorbeck D, et al. Dual targeting of hepatic fibrosis and atherogenesis by icosabutate, an engineered eicosapentaenoic acid derivative. *Liver Int* 2020; 40: 2860-76.
- Ji T, Feng W, Zhang X, et al. HDAC inhibitors promote pancreatic stellate cell apoptosis and relieve pancreatic fibrosis by upregulating miR-15/16 in chronic pancreatitis. *Hum Cell* 2020; 33: 1006-16.
- Price RG, Wong M. Heterogeneity of goodpasture's antigen. *J Pathol* 1988; 156: 97-9.
- Wang J, Xu Y, Jing H, et al. ROR $\gamma$  inhibitor SR1001 alleviates acute pancreatitis by suppressing pancreatic IL-17-producing Th17 and  $\gamma$ delta-T cells in mice with ceruletide-induced pancreatitis. *Basic Clin Pharmacol Toxicol* 2021; 129: 357-68.
- Rongione AJ, Kusske AM, Kwan K, et al. Interleukin 10 reduces the severity of acute pancreatitis in rats. *Gastroenterology* 1997; 112: 960-7.
- Lankisch PG, Apte M, Banks PA. Acute pancreatitis. *Lancet* 2015; 386: 85-96.
- Peery AF, Dellon ES, Lund J, et al. Burden of gastrointestinal disease in the United States: 2012 update. *Gastroenterology* 2012; 143: 1179-87 e3.
- Piersma B, Hayward MK, Weaver VM. Fibrosis and cancer: a strained relationship. *Biochim Biophys Acta Rev Cancer* 2020; 1873: 188356.
- Cheng Q, Wang L. LncRNA XIST serves as a ceRNA to regulate the expression of ASF1A, BRWD1M, and PFKFB2 in kidney transplant acute kidney injury via sponging hsa-miR-212-3p and hsa-miR-122-5p. *Cell Cycle* 2020; 19: 290-9.
- Calatayud D, Dehlendorff C, Boisen MK, et al. Tissue MicroRNA profiles as diagnostic and prognostic biomarkers in patients with resectable pancreatic ductal adenocarcinoma and periampullary cancers. *Biomark Res* 2017; 5: 8.

25. Zhang X, Lu J, Zhang Q, Luo Q, Liu B. CircRNA RSF1 regulated ox-LDL induced vascular endothelial cells proliferation, apoptosis and inflammation through modulating miR-135b-5p/HDAC1 axis in atherosclerosis. *Biol Res* 2021; 54: 11.
26. Hao Y, Miao J, Liu W, et al. Mesenchymal stem cell-derived exosomes carry microRNA-125a to protect against diabetic nephropathy by targeting histone deacetylase 1 and downregulating endothelin-1. *Diabetes Metab Syndr Obes* 2021; 14: 1405-18.
27. Sun Y, Wang H, Li Y, et al. miR-24 and miR-122 negatively regulate the transforming growth factor-beta/smad signaling pathway in skeletal muscle fibrosis. *Mol Ther Nucleic Acids* 2018; 11: 528-37.
28. Harms D, Choi M, Allers K, et al. Specific circulating microRNAs during hepatitis E infection can serve as indicator for chronic hepatitis E. *Sci Rep* 2020; 10: 5337.
29. Hartman H, Wetterholm E, Thorlacius H, Regner S. Histone deacetylase regulates trypsin activation, inflammation, and tissue damage in acute pancreatitis in mice. *Dig Dis Sci* 2015; 60: 1284-9.
30. Wang W, Liu Y, Zhao L. Tambulin targets histone deacetylase 1 inhibiting cell growth and inducing apoptosis in human lung squamous cell carcinoma. *Front Pharmacol* 2020; 11: 1188.
31. Deng X, He Y, Miao X, Yu B. ATF4-mediated histone deacetylase HDAC1 promotes the progression of acute pancreatitis. *Cell Death Dis* 2021; 12: 5.
32. Cao LL, Song X, Pei L, et al. Histone deacetylase HDAC1 expression correlates with the progression and prognosis of lung cancer: A meta-analysis. *Medicine (Baltimore)* 2017; 96: e7663.
33. Zhang W, Zhang Y, Tu T, et al. Dual inhibition of HDAC and tyrosine kinase signaling pathways with CUDC-907 attenuates TGFbeta1 induced lung and tumor fibrosis. *Cell Death Dis* 2020; 11: 765.
34. Rubio K, Singh I, Dobersch S, et al. Inactivation of nuclear histone deacetylases by EP300 disrupts the MiCEE complex in idiopathic pulmonary fibrosis. *Nat Commun* 2019; 10: 2229.
35. Pan X, Fang X, Wang F, et al. Butyrate ameliorates caerulein-induced acute pancreatitis and associated intestinal injury by tissue-specific mechanisms. *Br J Pharmacol* 2019; 176: 4446-61.
36. Cui H, Jiang D, Banerjee S, et al. Monocyte-derived alveolar macrophage apolipoprotein E participates in pulmonary fibrosis resolution. *JCI Insight* 2020; 5: e134539.
37. Huebbe P, Rimbach G. Evolution of human apolipoprotein E (APOE) isoforms: gene structure, protein function and interaction with dietary factors. *Ageing Res Rev* 2017; 37: 146-61.
38. Khalil YA, Rabes JP, Boileau C, Varret M. APOE gene variants in primary dyslipidemia. *Atherosclerosis* 2021; 328: 11-22.
39. Du S, Wang H, Cai J, et al. Apolipoprotein E2 modulates cell cycle function to promote proliferation in pancreatic cancer cells via regulation of the c-Myc-p21(Waf1) signalling pathway. *Biochem Cell Biol* 2020; 98: 191-202.
40. Shi Y, Yamada K, Liddel SA, et al. ApoE4 markedly exacerbates tau-mediated neurodegeneration in a mouse model of tauopathy. *Nature* 2017; 549: 523-7.
41. Safieh M, Korczyn AD, Michaelson DM. ApoE4: an emerging therapeutic target for Alzheimer's disease. *BMC Med* 2019; 17: 64.